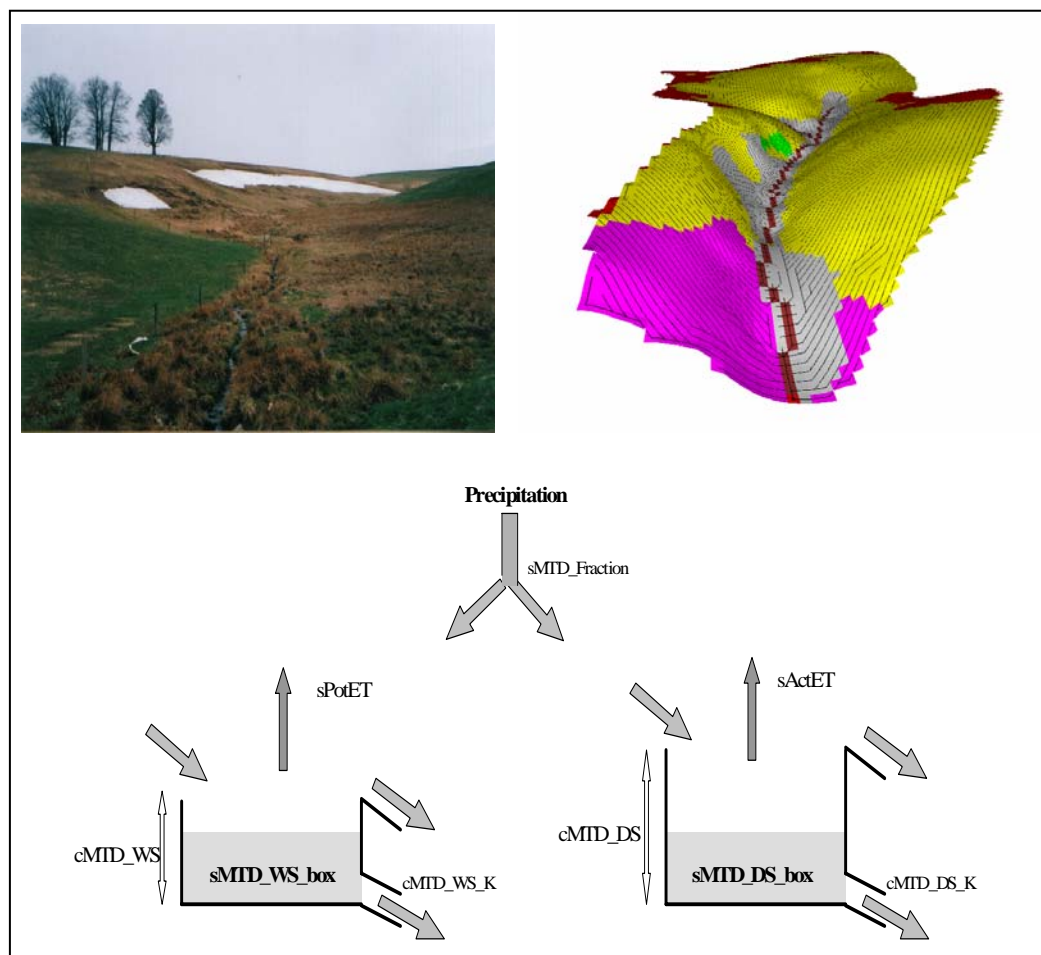


# Runoff generation in the riparian area of the Haldenbach micro-catchment (Germany)

*Development of the spatial variable riparian area module (SVRA-module) for the Distributed Tracer Aided Catchment model (TAC-D)*

A.J. Menkveld



April 2003



WAGENINGEN UNIVERSITY  
ENVIRONMENTAL SCIENCES



Institut für Hydrologie  
Albert-Ludwigs-Universität Freiburg

# Runoff generation in the riparian area of the Haldenbach micro-catchment (Germany)

*Development of the spatial variable riparian area module (SVRA-module)  
for the Distributed Tracer Aided Catchment model (TAC-D)*

A.J. Menkveld  
(reg. nr. 780829557040)

Wageningen, 2003

MSc thesis Hydrology (K150-717)

Under supervision of:

dr. ir. H.A.J. van Lanen (Wageningen University)

dr. S. Uhlenbrook (Albert Ludwig Universität Freiburg)

## Preface

---

For this research I spent 3 months in Freiburg i. Br. at the Institut für Hydrologie. I had a very good time there and I want to thank all thesis students and staff at the institute for that. I especially want to thank my supervisor there, Stefan Ulhenbrook, for his suggestions for my research and also Bettina Ott who helped me a lot with exploring the model. Also a special thanks to my other supervisor Henny van Lanen, for all his good ideas and support and for his visit to Freiburg.

The research did not always go the way I wanted and there were times I would do anything to get rid of it, especially when the model was not doing what I wanted it to do and nobody could help me with it. I would like to thank my friends and family and the thesis students from the sub-department of Water Resources in Wageningen for cheering me up when I was down. A special thanks hereby to Arjan van 't Zelfde because of his support in Freiburg and in Wageningen.

For several reasons this reasearch took more time than estimated, however, looking back, I can say that I learned a lot of this research and not only technical things but also a lot about myself.

Anja Menkveld  
14 April, 2003

## Table of Contents

---

<b>TABLE OF CONTENTS.....</b>	<b>I</b>
<b>TABLE OF FIGURES.....</b>	<b>III</b>
<b>TABLE OF TABLES.....</b>	<b>V</b>
<b>SUMMARY.....</b>	<b>VI</b>
<b>1. INTRODUCTION.....</b>	<b>1</b>
<b>2. AREA DESCRIPTION.....</b>	<b>3</b>
2.1. LOCATION AND CHARACTERISTICS OF THE MICRO-CATCHMENT .....	3
2.1.1. <i>Characteristics of the Brugga catchment</i> .....	3
2.1.2. <i>Selection criteria for the micro-catchment</i> .....	3
2.1.3. <i>Location of the micro-catchment</i> .....	3
2.1.4. <i>Characteristics of the riparian area</i> .....	5
2.2. TOPOGRAPHY, GEOLOGY, SOIL AND LAND USE .....	7
2.2.1. <i>Topography</i> .....	7
2.2.2. <i>Geology</i> .....	7
2.2.3. <i>Soil characteristics</i> .....	8
2.2.4. <i>Land use</i> .....	8
2.3. CLIMATE AND HYDROLOGY .....	8
2.3.1. <i>Climate</i> .....	8
2.3.2. <i>Hydrology</i> .....	9
<b>3. METHODS .....</b>	<b>11</b>
3.1. DESCRIPTION OF THE DYNAMIC GIS-PROGRAM PCRASTER .....	11
3.1.1. <i>Basic concept</i> .....	11
3.1.2. <i>Structure of Dynamic Modelling</i> .....	12
3.2. DESCRIPTION OF THE MODEL TAC-D.....	13
3.2.1. <i>Introduction</i> .....	13
3.2.2. <i>Model outlook</i> .....	14
3.2.3. <i>Local drain direction network</i> .....	15
3.2.4. <i>Lateral flows</i> .....	16
3.2.5. <i>Snow routine</i> .....	16
3.2.6. <i>Soil routine</i> .....	17
3.2.7. <i>Runoff generation module</i> .....	17
3.2.8. <i>Stream cells</i> .....	19
3.2.9. <i>Urban areas</i> .....	19
3.2.10. <i>Wave building</i> .....	19
3.2.11. <i>Climatic input data</i> .....	19
3.2.12. <i>Flow chart of the TAC-D model</i> .....	20
3.3. SILICA AS A GEOLOGICAL TRACER .....	22
3.3.1. <i>Introduction to Silica</i> .....	22
3.3.2. <i>Silica concentrations in the Brugga catchment</i> .....	22
<b>4. INPUT DATA AND MAPS FOR APPLYING TAC-D TO THE HALDENBACH MICRO-CATCHMENT .....</b>	<b>24</b>
4.1. EXISTING DATA.....	24
4.2. PRE-PROCESSING OF THE SPATIAL DATA .....	24

4.2.1. <i>Digital Elevation Model</i> .....	24
4.2.2. <i>Map of zones with dominant runoff generation processes</i> .....	24
4.2.3. <i>Other maps</i> .....	25
4.3. PRE-PROCESSING OF THE NON-SPATIAL DATA.....	25
4.3.1. <i>Rain data</i> .....	25
4.3.2. <i>Discharge</i> .....	25
4.3.3. <i>Air temperature</i> .....	26
4.3.4. <i>Sunshine duration</i> .....	26
4.3.5. <i>Wind speed and humidity</i> .....	26
4.3.6. <i>Silica concentrations</i> .....	27
4.4. INITIAL WATER STORAGE.....	27
4.5. TIME DISCRETIZATION .....	28
4.5.1. <i>Modelling period</i> .....	28
4.5.2. <i>Initialisation</i> .....	28
4.5.3. <i>Calibration and Validation period</i> .....	28
4.6. CRITERIA FOR MODEL PERFORMANCE .....	28
<b>5. EXTENSIONS TO TAC-D</b> .....	<b>30</b>
5.1. WATER BALANCE CHECK.....	30
5.2. SPATIAL VARIABILITY OF THE RIPARIAN AREA (SVRA-MODULE) .....	30
5.2.1. <i>Concept of the riparian area</i> .....	30
5.2.2. <i>The former MTD concept</i> .....	30
5.2.3. <i>The new MTD concept</i> .....	30
5.3. INTEGRATION OF SILICA IN THE REVISED TAC-D MODEL .....	33
5.3.1. <i>Introduction to the silica module</i> .....	33
5.3.2. <i>Concept of the silica module</i> .....	33
<b>6. RESULTS</b> .....	<b>35</b>
6.1. ORIGINAL TAC-D MODEL .....	35
6.2. REVISED TAC-D MODEL WITH THE SPATIALLY VARIABLE RIPARIAN AREA MODULE .....	37
6.3. ENLARGED BASE FLOW .....	38
<b>7. PARAMETER SENSITIVITY ANALYSIS</b> .....	<b>40</b>
7.1. PROCEDURE .....	40
7.2. RESULTS .....	40
<b>8. MODEL UPSCALING</b> .....	<b>43</b>
8.1. INTRODUCTION .....	43
8.2. SPATIAL RESOLUTION FROM 5X5 M TO 50X50 M .....	43
8.3. RESULTS .....	44
<b>9. RESULTS OF THE SILICA MODULE</b> .....	<b>46</b>
9.1. SIMULATED SILICA CONCENTRATIONS .....	46
9.2. SENSITIVITY OF THE SILICA MODULE .....	46
<b>10. CONCLUSIONS AND RECOMMENDATIONS</b> .....	<b>48</b>
<b>REFERENCES</b> .....	<b>50</b>
<b>ANNEXES</b> .....	<b>52</b>

# 1. Introduction

## ***Aim of the study***

The development of catchment models is done to gain more insight in the relevant water flow processes. This understanding is important, for example, to prevent floods and droughts or to predict the water quality. In Germany, a lot of research has already been done on the topic of catchment modelling (e.g. Uhlenbrook, 1999; Hoeg, S. *et al.*, 2000). The Institut für Hydrologie of the Albert-Ludwigs-Universität Freiburg is specialised in the use of tracer data to increase the knowledge of the runoff generation in a catchment. By using tracer data, the process oriented modelling can be improved. In Freiburg, this is being done by developing the process oriented model TAC-D (Distributed Tracer Aided Catchment model) (Roser *et al.*, 2001).

The TAC-D model was developed in 1999 as an extension to the TAC-model (Uhlenbrook, 1999), which is a semi-distributed runoff generation model. The TAC-D model was developed to improve the conceptualisation of the different runoff generation zones and to integrate new process knowledge into the runoff generation module, representing zones having the same dominant runoff processes. TAC-D was integrated into a dynamic GIS, named PCRaster (PCRaster team, unknown year). The result of this integration was that the model became distributed and the resulting spatial discretization was used for the new runoff generation module. The developed model was implemented to the Brugga catchment. The implementation was successful and the results were very good. In the one-year calibration period, a model efficiency ( $R_{\text{eff}}$ ) of 0.94 was reached and in the three-year validation period, a  $R_{\text{eff}}$  of 0.80 was reached. For a sub-catchment of the Brugga, the St Wilhelmer Talbach, the model efficiency was a bit less, but still good, with  $R_{\text{eff}} = 0.85$  and  $R_{\text{eff}} = 0.77$ , for the calibration and validation period, respectively.

The modelling of the riparian area (saturated areas connected to the stream) in the runoff generation module, was expected to leave space for improvement. The various processes in these zones are not sufficiently elaborated yet to receive satisfying results. Therefore, a micro-catchment with a relatively high percentage of riparian area was selected to revise TAC-D. In this micro-catchment, called the Haldenbach catchment, measurements were taken during the autumn of 1999 (Sieder *et al.*, 2000). The data collected during this period will be used in this research.

The aim of this study is to develop a process oriented runoff generation module for the riparian area, within the framework of the catchment model TAC-D. This module aims at a representation of the spatial variability of the riparian area and to integrate silica concentrations, as a tracer, into the module. Incorporation of silica is meant to examine which runoff generation zones contribute in which amount to the generated runoff. Furthermore, the sensitivity of the parameters used in the module was investigated, by conducting a parameter sensitivity analysis. Finally, a research was carried out to investigate the effect of a larger spatial resolution (upscaling) on the model performance.

## ***Research approach***

To reach the goal of this study, various steps were identified. First all input data, consisting of the measured runoff and climate data was pre-processed, to the appropriate time scale. Furthermore, PCRaster maps used in TAC-D, for example, with land use, location of the stream or slope were compiled. These input data for the Haldenbach micro-catchment was entered into the model. As a next step, a module was developed to conceptualise the riparian area; i.e. the spatially variable riparian area module (SVRA-module). The SVRA-module divides the riparian area into fully saturated areas and semi-dry areas.

In addition, a module was developed to simulate the silica concentrations in the stream. This module was integrated in the SVRA-module. With this extended SVRA-module was investigated which zone is contributing to the runoff and in what amount. After this, a parameter sensitivity analysis of revised module was executed.

Finally, the raster of the model was scaled up to a larger spatial resolution and the model performance from both the SVRA-module with a small and a large resolution were compared. The expected effect of upscaling is that spatial details cannot be incorporated in the model and therefore relevant information is lost. The advantage of upscaling is that calculation time is reduced and less spatial data is required, which is especially relevant for larger catchments.

### ***Report set up***

In Chapter 2, a description of the area is given, containing the location and characteristics of the micro-catchment. A subchapter about the topography, geology, soil and land use is also incorporated in this chapter. Finally, climate and hydrology are dealt with here. In Chapter 3, the methods used in this research are described. First a description of the dynamic GIS-program PCRaster is given, followed by a description of TAC-D. At the end of the chapter, a paragraph is included about silica as a geological tracer. A description of all the input data is given in Chapter 4. Chapter 5 describes the extensions made to TAC-D and includes the concept to the SVRA-module and the silica module. In Chapter 6, the results of the application of the different modules to the Haldenbach micro-catchment are presented. Chapter 7 describes the results of the parameter sensitivity analysis, which was carried out for the SVRA-module. The upscaling of the area is described in Chapter 8, and Chapter 9 describes the output of the silica module. In the final chapter, Chapter 10, conclusions are drawn and recommendations for further research are suggested.

## Table of Figures

---

<b>Figure 2.1</b>	The location of the Brugga catchment and the location of the Haldenbach micro-catchment
<b>Figure 2.2</b>	Location of the Haldenbach micro-catchment, riparian area and the Haldenbach (stream)
<b>Figure 2.3</b>	The Haldenbach micro-catchment with the riparian area in March and May 2002
<b>Figure 2.4</b>	Confluence of the two streams of the Haldenbach with organic bulges
<b>Figure 2.5</b>	Ideal layering of a periglacial cover
<b>Figure 2.6</b>	Rising water table caused by groundwater ridging: a) situation before precipitation and b) development of a groundwater ridge
<b>Figure 2.7</b>	Rising water table caused by piston-flow
<b>Figure 3.1</b>	Different attribute values of one cell stored in three map layers
<b>Figure 3.2</b>	Different levels of linkage between the model and the database
<b>Figure 3.3</b>	Schematic representation of a dynamic model
<b>Figure 3.4</b>	General storage concept of TAC-D
<b>Figure 3.5</b>	Different storage concepts used in TAC-D
<b>Figure 3.6</b>	Haldenbach micro-catchment in 3D, with the different runoff generation zones, the stream and the local drain direction network
<b>Figure 3.7</b>	Cascade of barrels
<b>Figure 3.8</b>	Assignment scheme for runoff generation zones
<b>Figure 3.9</b>	Storage concept of the different runoff generation zones in TAC-D
<b>Figure 3.10</b>	Concept of the stream cells
<b>Figure 3.11</b>	Flow diagram of TAC-D
<b>Figure 3.12</b>	Goldich weathering sequence
<b>Figure 4.1</b>	Runoff generation zones in the Haldenbach catchment
<b>Figure 4.2</b>	Sub-catchments of the Haldenbach micro-catchment
<b>Figure 4.3</b>	Precipitation and runoff in the Haldenbach micro-catchment
<b>Figure 4.4</b>	Measured silica concentrations and discharge at gauging station OM
<b>Figure 5.1</b>	Former MTD storage concept
<b>Figure 5.2</b>	New MTD storage concept
<b>Figure 5.3</b>	Revised flow diagram of TAC-D; SVRA-module is included
<b>Figure 5.4</b>	Concept of the silica module
<b>Figure 5.5</b>	Example of the silica module
<b>Figure 6.1</b>	Observed and simulated hydrographs with the original TAC-D model and original parameters
<b>Figure 6.2</b>	Observed and simulated hydrographs with the original TAC-D model and adjusted parameters
<b>Figure 6.3</b>	Observed and simulated hydrographs with the revised TAC-D model, including the SVRA-module
<b>Figure 6.4</b>	Calculated amount of rain from the runoff
<b>Figure 7.1</b>	Sensitivity of the storage capacity of the Wet Storage box of the riparian area on the simulated runoff
<b>Figure 7.2</b>	Sensitivity of the hydraulic conductivity of the deep groundwater on the simulated runoff
<b>Figure 8.1</b>	The original catchment (5 m cell length) and the new one (50 m cell length)
<b>Figure 8.2</b>	The new runoff generation zone map
<b>Figure 8.3</b>	Observed and simulated hydrographs with the revised TAC-D model, including the SVRA-module with parameters of the reference model and a cell length of 50 m



- Figure 8.4** Observed and simulated hydrographs with the revised TAC-D model, including the SVRA-module with parameters ten times smaller than the reference model and a cell length of 50 m
- Figure 9.1** Silica concentrations and discharge at gauging station OM
- Figure 9.2** Influence of the silica concentrations of the different boxes on the simulated silica concentrations at gauging station OM

## Table of Tables

---

<b>Table 2.1</b>	Area of the riparian areas in the Haldenbach micro-catchment
<b>Table 3.1</b>	Characteristics of the different flow systems
<b>Table 4.1</b>	Changed area caused by digitalizing the micro-catchment
<b>Table 6.1</b>	Adjusted parameters for the Haldenbach micro-catchment
<b>Table 6.2</b>	Model efficiency and volume error of the original TAC-D model
<b>Table 6.3</b>	Adjusted parameters for the revised TAC-D model with the SVRA-module
<b>Table 6.4</b>	Model efficiency and volume error of the revised TAC-D model with the SVRA-module
<b>Table 7.1</b>	Results of the parameter sensitivity analysis of the SVRA-module
<b>Table 8.1</b>	Characteristics of the original area (cell size 5x5 m) and the upscaled area (cell size 50x50 m)
<b>Table 8.2</b>	Parameters of the 5 m cell length and the 50 m cell length module
<b>Table 8.3</b>	Performance of the model with a cell length of 5 and 50 m

## Summary

---

The aim of this study is the improvement of the modelling of the flow dynamics in the riparian areas within the Distributed Tracer Aided Catchment Model (TAC-D). Therefore, TAC-D is adjusted to incorporate a new module representing the riparian areas. The revised TAC-D including this new module was applied to the micro-catchment the Haldenbach in the Black Forest (Germany).

The original TAC-D was applied to a meso-scale catchment in the Black Forest, the Brugga catchment. For my research, data from the Haldenbach micro-catchment, a sub-catchment of the Brugga, was used. These data was obtained from 21 October – 6 November 1999. The area of this micro-catchment is only 0.21 km<sup>2</sup> and the mean elevation is ca. 1100 m above m.s.l. The research area consists of flat hilltops, periglacial cover layers, not layered drift cover, moraines and a riparian area.

TAC-D is a conceptual model and is developed in the raster based program PCRaster. The basic concept of TAC-D is that for different runoff generation zones, different storage concepts are defined. These storage boxes receive water from upstream boxes, precipitation and water from soil moisture. The water from the boxes is routed to the deep groundwater box or to a downstream storage box. The different boxes form a cascade to the stream.

The concept of the riparian area in the original TAC-D was represented with one box. This box has a potential evaporation and a limited storage capacity, to represent the saturated status of the riparian area. Field observations in May 2002 showed that the riparian area is not completely saturated but dry organic bulges are also present in the area. Therefore, the concept, in this study, was changed into 2 boxes for the riparian area; a Wet Storage box, with a small storage capacity and always potential evaporation, and a Dry Storage box, with a larger storage capacity and actual evaporation from the box. The area of the wet and dry zone is not constant, but varies with time dependent on the water stored in the Wet Storage box. Instead of changing the wet and dry areas in the model only the amounts of water routed to the Wet and Dry Storage box were changed.

The original TAC-D with calibrated parameters for the Haldenbach micro-catchment lead to reasonable results (model efficiency: 36%). However, there was space for improvement and therefore the model was adjusted to include the new riparian area concept. The new module was called the spatial variable riparian area module (SVRA-module). The application of TAC-D including this SVRA-module shows good results (model efficiency: 93%).

A parameter sensitivity analysis was also carried out in this research. The main conclusion was that the hydraulic conductivity has a large effect on the amount of simulated runoff and that these conductivity's are very scale dependent.

Upscaling, with the revised TAC-D model, to a larger spatial resolution was also performed. The advantages of upscaling are that calculation time is reduced and less spatial data is needed, which is especially important for larger catchments. The cell size used for the Haldenbach micro-catchment was enlarged from 5x5 m to 50x50 m. Consequently, a new calibration was necessary, because the amount of cells was reduced from ca. 9000 to nearly 90 cells. The hydraulic conductivity's had to be 10 times smaller to reflect the time that the water needs to reach the outlet. With these calibrated parameters the results were still not satisfying, because this larger spatial resolution does not represent the micro-scale processes correctly.

For this research also a silica-module was developed. The aim of this module is to create another validation possibility for the flow in the different runoff generation zone. Each storage was assigned a silica concentration and this module was integrated into TAC-D including the SVRA-module. Unfortunately this module was not working as expected. The concentrations in the stream became too low after a discharge peak and the recovery of the concentration in the base flow was too slow. These deviations are the result of the chosen concept. The concept states that each box has its own concentration and the mixing of the concentrations only takes place outside the boxes. Probably, mixing inside the boxes is necessary to simulate the concentration in the stream.

In conclusion, the newly developed SVRA-module gives good results when it is applied to the Haldenbach micro-catchment. The model, however, is very scale dependent and the parameter values have no physical meaning. Therefore, a new calibration is necessary when TAC-D is applied to another catchment. The main use of TAC-D, including the SVRA-module, after calibration, is therefore to gain a better understanding of the hydrological processes that take place in a catchment. For predictions of the behaviour of the catchment with changing catchment characteristics (e.g. drainage in the catchment) this model is not suitable.

# 1. Introduction

## ***Aim of the study***

The development of catchment models is done to gain more insight in the relevant water flow processes. This understanding is important, for example, to prevent floods and droughts or to predict the water quality. In Germany, a lot of research has already been done on the topic of catchment modelling (e.g. Uhlenbrook, 1999; Hoeg, S. *et al.*, 2000). The Institut für Hydrologie of the Albert-Ludwigs-Universität Freiburg is specialised in the use of tracer data to increase the knowledge of the runoff generation in a catchment. By using tracer data, the process oriented modelling can be improved. In Freiburg, this is being done by developing the process oriented model TAC-D (Distributed Tracer Aided Catchment model) (Roser *et al.*, 2001).

The TAC-D model was developed in 1999 as an extension to the TAC-model (Uhlenbrook, 1999), which is a semi-distributed runoff generation model. The TAC-D model was developed to improve the conceptualisation of the different runoff generation zones and to integrate new process knowledge into the runoff generation module, representing zones having the same dominant runoff processes. TAC-D was integrated into a dynamic GIS, named PCRaster (PCRaster team, unknown year). The result of this integration was that the model became distributed and the resulting spatial discretization was used for the new runoff generation module. The developed model was implemented to the Brugga catchment. The implementation was successful and the results were very good. In the one-year calibration period, a model efficiency ( $R_{\text{eff}}$ ) of 0.94 was reached and in the three-year validation period, a  $R_{\text{eff}}$  of 0.80 was reached. For a sub-catchment of the Brugga, the St Wilhelmer Talbach, the model efficiency was a bit less, but still good, with  $R_{\text{eff}} = 0.85$  and  $R_{\text{eff}} = 0.77$ , for the calibration and validation period, respectively.

The modelling of the riparian area (saturated areas connected to the stream) in the runoff generation module, was expected to leave space for improvement. The various processes in these zones are not sufficiently elaborated yet to receive satisfying results. Therefore, a micro-catchment with a relatively high percentage of riparian area was selected to revise TAC-D. In this micro-catchment, called the Haldenbach catchment, measurements were taken during the autumn of 1999 (Sieder *et al.*, 2000). The data collected during this period will be used in this research.

The aim of this study is to develop a process oriented runoff generation module for the riparian area, within the framework of the catchment model TAC-D. This module aims at a representation of the spatial variability of the riparian area and to integrate silica concentrations, as a tracer, into the module. Incorporation of silica is meant to examine which runoff generation zones contribute in which amount to the generated runoff. Furthermore, the sensitivity of the parameters used in the module was investigated, by conducting a parameter sensitivity analysis. Finally, a research was carried out to investigate the effect of a larger spatial resolution (upscaling) on the model performance.

## ***Research approach***

To reach the goal of this study, various steps were identified. First all input data, consisting of the measured runoff and climate data was pre-processed, to the appropriate time scale. Furthermore, PCRaster maps used in TAC-D, for example, with land use, location of the stream or slope were compiled. These input data for the Haldenbach micro-catchment was entered into the model. As a next step, a module was developed to conceptualise the riparian area; i.e. the spatially variable riparian area module (SVRA-module). The SVRA-module divides the riparian area into fully saturated areas and semi-dry areas.

In addition, a module was developed to simulate the silica concentrations in the stream. This module was integrated in the SVRA-module. With this extended SVRA-module was investigated which zone is contributing to the runoff and in what amount. After this, a parameter sensitivity analysis of revised module was executed.

Finally, the raster of the model was scaled up to a larger spatial resolution and the model performance from both the SVRA-module with a small and a large resolution were compared. The expected effect of upscaling is that spatial details cannot be incorporated in the model and therefore relevant information is lost. The advantage of upscaling is that calculation time is reduced and less spatial data is required, which is especially relevant for larger catchments.

### ***Report set up***

In Chapter 2, a description of the area is given, containing the location and characteristics of the micro-catchment. A subchapter about the topography, geology, soil and land use is also incorporated in this chapter. Finally, climate and hydrology are dealt with here. In Chapter 3, the methods used in this research are described. First a description of the dynamic GIS-program PCRaster is given, followed by a description of TAC-D. At the end of the chapter, a paragraph is included about silica as a geological tracer. A description of all the input data is given in Chapter 4. Chapter 5 describes the extensions made to TAC-D and includes the concept to the SVRA-module and the silica module. In Chapter 6, the results of the application of the different modules to the Haldenbach micro-catchment are presented. Chapter 7 describes the results of the parameter sensitivity analysis, which was carried out for the SVRA-module. The upscaling of the area is described in Chapter 8, and Chapter 9 describes the output of the silica module. In the final chapter, Chapter 10, conclusions are drawn and recommendations for further research are suggested.

## 2. Area description

In this chapter, the different characteristics of the micro-catchment are described. The information is mainly derived from Sieder *et al.* (2000), who carried out a research in the micro-catchment during the autumn of 1999. First some characteristics of the larger Brugga catchment are described, subsequently the selection criteria for the micro-catchment are explained.

### 2.1. Location and characteristics of the micro-catchment

#### 2.1.1. Characteristics of the Brugga catchment

The micro-catchment (Haldenbach catchment) is a small sub-catchment of the Brugga catchment. The Brugga catchment is situated in the southern part of the Black Forest in Germany, near Freiburg (Figure 2.1). The catchment has an area of 40 km<sup>2</sup> and has large elevation differences. The outlet is situated at 434 m above mean sea level (m.s.l.), the highest point of the catchment is the Feldberg at 1493 meter above m.s.l.. The Brugga catchment consists of three morphological units:

- flat hilltops (20% of the area), which are the remains of Permian or Tertiary topography
- steep hill slopes with a slope > 50° (75% of the area)
- weakly developed valley soils (5% of the area) in the U- and V-valley's

A more detailed description can be found in Uhlenbrook (1999).

#### 2.1.2. Selection criteria for the micro-catchment

The Haldenbach<sup>1</sup> catchment was selected based on the following criteria (Sieder *et al.*, 2000):

- sub-catchment of the Brugga;
- high percentage of riparian area in direct contact with a stream;
- saturated status of the riparian area in the micro-catchment;
- measurable runoff in the stream;
- good accessibility;
- approval of the land owners for the research, and
- representative for the other riparian areas in the Brugga catchment.

#### 2.1.3. Location of the micro-catchment

The micro-catchment is situated in the Brugga catchment, at the border of the western catchment near Schauinsland (Figure 2.1). The Haldenbach catchment is positioned between the street L124 and the Bodenmattenweg (Figure 2.2). The Haldenbach is lead trough a pipe under the latter road. Just before the entrance of this pipe, a gauging station was installed, defining the downstream border of the catchment for this research. This gauging station was named MU (Messwehr Unter<sup>2</sup>), so the catchment area of the Haldenbach is also referred to as catchment MU. The Haldenbach rises in a spring at 1128 m above m.s.l., the gauging station (MU) was installed at a height of 1078 m above m.s.l.. During the research, another gauging station was installed in the stream; the gauging station OM (Obere Messwehr<sup>3</sup>), which is at 115 m upstream of MU. In between these two gauging stations a small sub-catchment occurs, i.e. catchment MU-OM. In Annex A, specific characteristics of the whole micro-catchment and the whole sub-catchments can be found. For example, the area of the total catchment is 0.21 km<sup>2</sup>.

---

<sup>1</sup> English: Halden brook

<sup>2</sup> English: lower gauging station

<sup>3</sup> English: upper gauging station

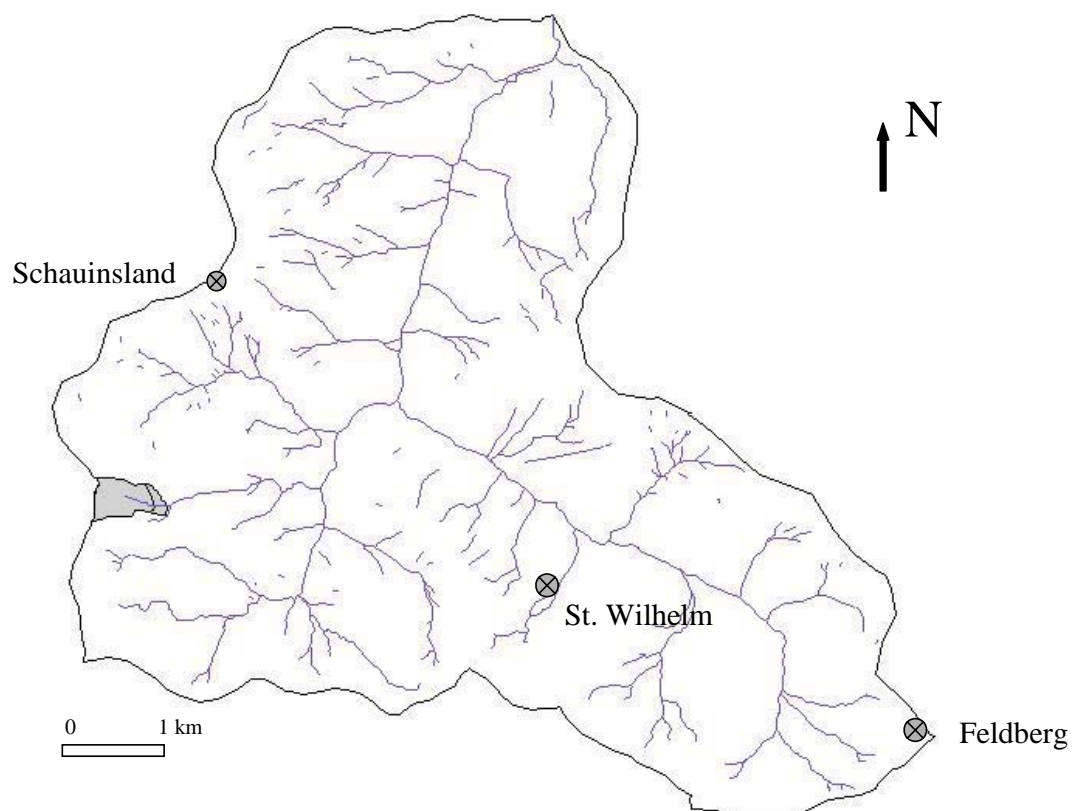
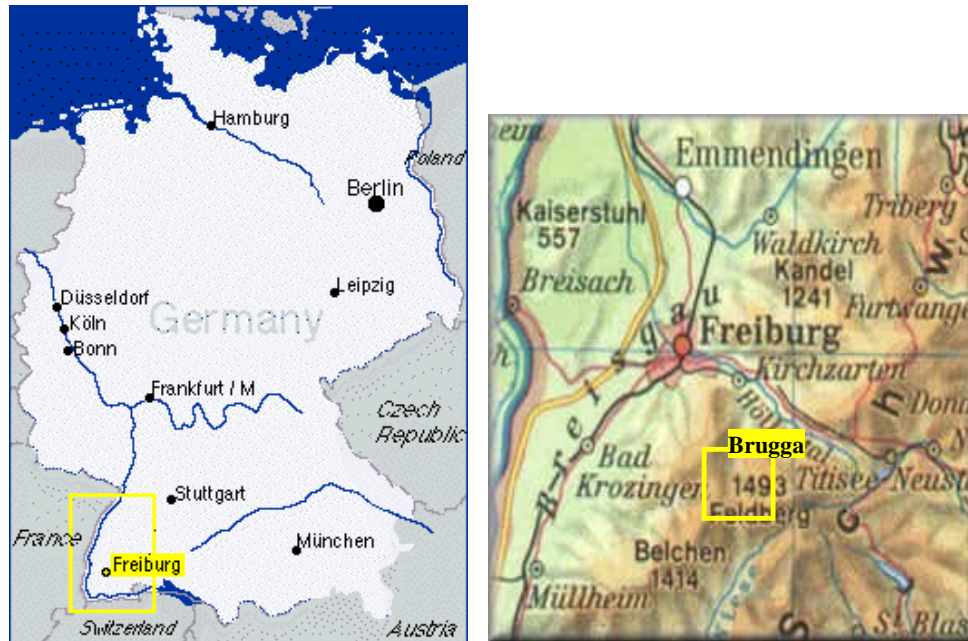


**Figure 2.1 The location of the Brugga catchment and the location of the Haldenbach micro-catchment**



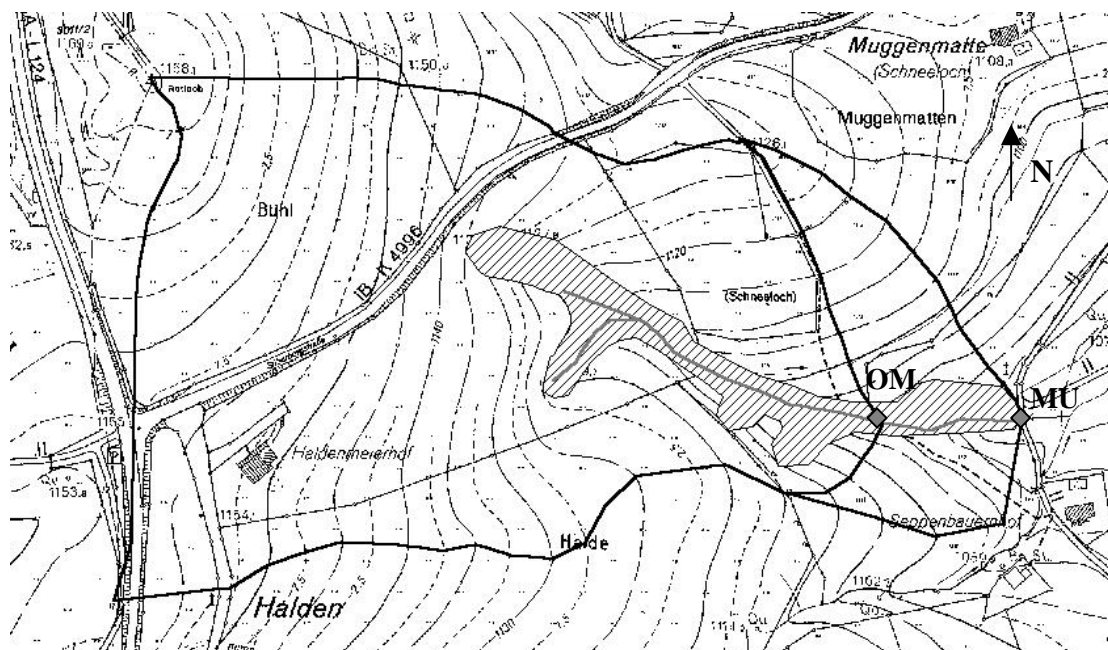


**Figure 2.2 Location of the Haldenbach micro-catchment, riparian area (dashed area) and the Haldenbach (stream)**

#### 2.1.4. Characteristics of the riparian area

The riparian area has a typical soil and vegetation. The nearly saturated soil has a high water-holding capacity. Pipes, sedge and other wet vegetation are specific for the saturated soil. Clearly recognisable in the field is the rather sharp transition from nearly, permanently, saturated soils to drier soils, through a change in vegetation (Figure 2.3). Table 2.1 gives a description of the area of the riparian areas in the sub-catchments and in the whole micro-catchment.

**Table 2.1 Area of the riparian areas in the Haldenbach micro-catchment**

Area of the Haldenbach micro-catchment	Catchment		
	MU	OM	MU-OM
<i>area [m<sup>2</sup>]</i>	208.000	181.000	27.000
<i>riparian area [m<sup>2</sup>]</i>	17.020	13.650	3.360
<i>percentage of catchment [%]</i>	8,2	7,5	12,5
<i>percentage of total riparian area [%]</i>	100	80	20

The riparian area is (nearly) saturated, although within the riparian area dry organic bulges occur. When pressure is exerted on the nearly saturated wet zone, water flows out. Dry bulges (Figure 2.4) have a different vegetation than the adjacent wet soil and no water flows out when pressure is exerted.

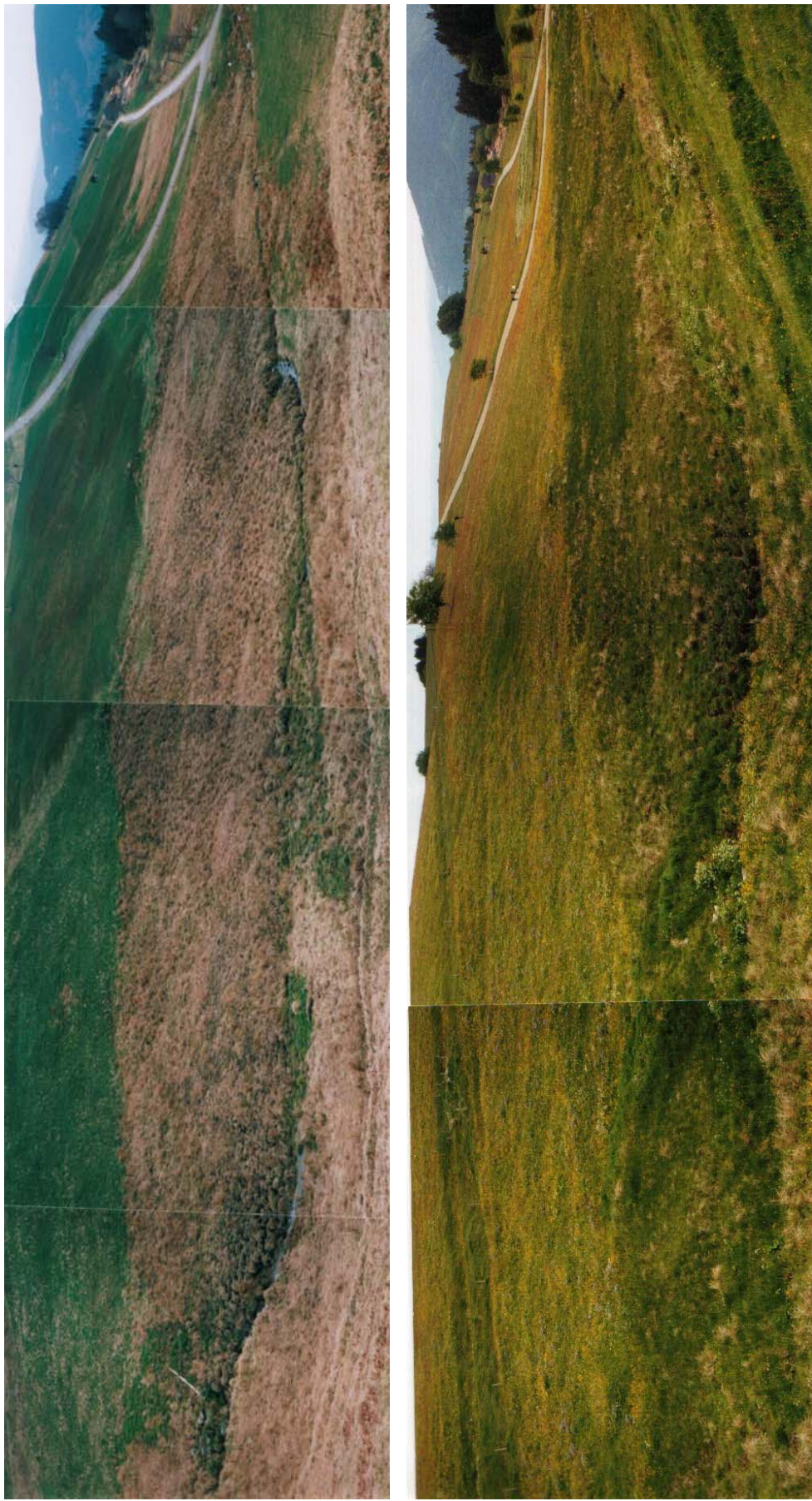


**Figure 2.3 The Haldenbach micro-catchment with the riparian area in March (above) and May (below) 2002**





**Figure 2.4 Confluence of the two streams of the Haldenbach with organic bulges**

The flow patterns in the riparian area are very complex, which can be derived from the measured EC (electric conductivity). Field observations in May 2002 showed that the EC can vary within a few decimetres distance from 100  $\mu\text{Si}/\text{cm}$  to 20  $\mu\text{Si}/\text{cm}$ .

## **2.2. Topography, Geology, Soil and Land use**

### **2.2.1. Topography**

The Haldenbach micro-catchment consists mainly of flat hilltops. In the lower part of the area, the southern slope is relative steep (a slope of 23%) and short. This slope becomes less steep after a twist. Less steep is the northern slope (max 10%) and it has no twist in it. In the lowest part, the valley becomes wider and the slopes are less steep. In the upper part of the catchment, a little man-made lake is situated.

### **2.2.2. Geology**

The micro-catchment is situated at the border of the Central Black Forest area with gneiss-anatexit mountains. The subsoil is predominated by metatexiten. The most common minerals are quarts, feldspars and biotite (hornblende). These minerals have their origin in the Precambrian sediments. In Upper Carboniferous, ore-tunnels were developed. At the same time, the mountains started to form cracks caused by the Varisian orogenesis. One of the ore tunnels might cross the micro-catchment. This tunnel was used in the Middle Ages for the exploitation of lead-zinc-ore. This can have an effect on the water quality in the area and might explain why the water has such a high chloride-level, caused by the presence of the mineral pyromorphit  $[\text{Pb}_5(\text{PO}_4)_3\text{Cl}]$ .

During the Tertiary the current relief developed. Then, the tectonic uplifted Black Forest (Alpine orogenesis), was largely affected by erosion. The warm climate in the Tertiary caused an immense oxidation of the weathering zones. During the Würm ice age, the glaciers reached the area around Schauinsland (Figure 2.1). This explains why around gauging station MU rests of moraine can be found. However, because of the short transportation path of the glaciers, the moraines do not vary much from the bedrock. The moraines are only 1-3 meters

thick and not so clayey as one might expect. On the slopes, the till is eroded and the underlying periglacial layer is now at the surface.

Before the glaciers came, there was a long periglacial period. In general, during this phase the following soil layers were formed through solifluction processes (Roser *et al.*, 2001):

- a weathering layer, where the bedrock is fragmented through physical and chemical weathering, but is not transported through erosion processes because of the ice cover;
- a base layer, which is layered parallel to the slope;
- a main layer with large boulders, and
- a cover layer.

In the Haldenbach micro-catchment no cover layer is formed. All layers together are 1-2 m thick. Figure 2.5 shows the ideal layering of a periglacial cover.

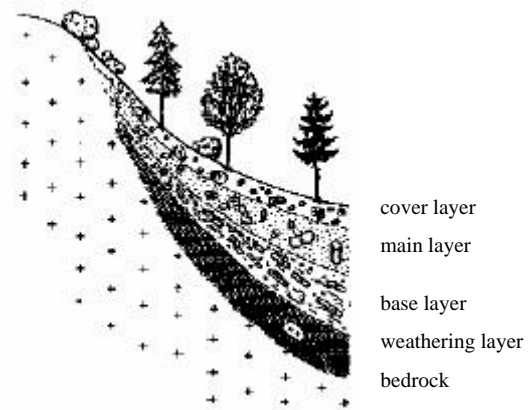


**Figure 2.5 Ideal layering of a periglacial cover (Rehfuess *fide* Roser, 2001)**

### 2.2.3. Soil characteristics

On the slopes Brown Forest soils occur. Depending on the thickness of the soil layer and the underlying parent material, the soil has a field capacity between 50 and 220 mm. The infiltration capacity is very high. In the saturated areas Gley soils can be found. These soils have a high amount of organic matter and the ions occur in a reduced form.

### 2.2.4. Land use

In Haldenbach micro-catchment, the land use is pastureland. During the summer the grass is harvested and cattle is grazing the area. A micro-topography in the riparian area is developed by the poaching of the grass sod.

The amount of urban (sealed) area is very low (4%), only one road crosses the area and there is one farm (Figure 2.2). Upstream of the Haldenbach is a small artificial lake (ca. 200 m<sup>2</sup>), which is fed by a spring. From this lake, one branch of the Haldenbach originates.

## 2.3. Climate and Hydrology

### 2.3.1. Climate

The climate in the Haldenbach catchment is strongly influenced by the synclinal western winds. In turns, it is influenced by the sub-tropic warm air and the sub-polar cold air. Therefore, the climate belongs to the temperate-transition-zones climate group. Locally, the climate is strongly affected by the topography. The mean year temperature at station Schauinsland (1218 above m.s.l.) is 4.8 °C. There the yearly minimum temperature is -2 °C and the maximum temperature is 13 °C. The mean sunshine duration is 1519 hours per year. The precipitation is strongly influenced by the orographic effects, dominated by fronts coming from the west. During the summer period, this effect is less clear because of the convective processes. The mean yearly precipitation at Station Schauinsland is 1558 mm, with 706 mm in the hydrological winter. About 30-35% of the total precipitation falls as snow.

The potential evaporation (ET<sub>p</sub>) calculated for the Brugga lies between 587 mm/yr (1.6 mm/d, Turc-Wendling) and 625 mm/yr (1.7 mm/d, Penman-Monteith) (Roser *et al.*, 2001). Sieder *et al* (2000) also calculated the evaporation with Turc-Wendling and Penman-Monteith, for several days. For the 26 of October 1999, the calculated ET<sub>p</sub> was 1.92 mm/d (Turc-Wendling) and 1.23 mm/d when calculated with the equation of Penman-Monteith.

### 2.3.2. Hydrology

#### *Description of run-off processes in the riparian area*

The riparian area is the main interest of this research. Riparian areas can develop through (Sieder *et al.*, 2000):

- small permeability of the soil;
- high precipitation;
- high infiltration capacity of the surrounding soil;
- micro-relief (cow spurs), and
- fine-grained sediments deposited by the stream.

In saturated areas different runoff processes occur. In general, the discharge from the riparian area consists of the newly precipitated water and the old, already infiltrated water from earlier showers. The different processes, which generate runoff in the saturated areas, are described below:

Groundwater ridging: in areas where the capillary zone reaches the surface, groundwater ridges occur during a shower. These ridges cause that earlier stored water is being pressed out into the stream. (Figure 2.6).

Piston flow effect: infiltrating water in areas further away from the stream causes a higher pressure in the aquifer and this rising pressure level causes 'old' water to be pressed out of the aquifer and into the stream (Figure 2.7).

Lateral flow through the macro-pores: in the macro-pores a very quick response of the discharge to precipitation can take place (velocities of cm/s). Therefore, macro-pores are also of great relevance in the runoff generation processes, especially when the macro-pores are long, connected and widespread.

All these processes can occur individually or simultaneously.

Horton overland flow: this is not typical for the riparian area, but can also occur there. Horton defined overland flow as a situation that when the precipitation intensity is larger than the infiltration capacity of the soil, the remaining water will leave the area as overland flow. In reality this phenomenon only occurs on saturated soils, hard bedrock or sealed urban areas, so not as much as one would expect from the definition (Uhlenbrook & Leibundgut, 1997).

#### *Discharge*

Generally in the area, the highest discharge can be measured in April, after the snowmelt. The lowest discharge can be expected at the end of the summer in August or September, caused by the summer evapotranspiration. This causes a depletion of the soil moisture storage and falling of the water table. In the Haldenbach micro-catchment, no discharge data is available for a long period, because there is only data available from measurements during a short period in October and November 1999. These data will be described in Chapter 4.

#### *Hydrological processes in the Haldenbach micro-catchment*

The main conclusions from Sieder *et al.* (2000) were that the micro-catchment reacts very quickly on a rain shower. With a lag time of 1 to 2 hours after a shower the discharge rises. The recession follows almost directly after the end of the shower. The base flow, however, increases after a shower. How much the increase depends of the amount of soil moisture in the catchment. The larger the amount of soil moisture and the lower the storage capacity of the soil, the quicker the response of the base flow on the shower is.

The contribution of the direct runoff (water from the shower which contributes directly to the runoff) on the discharge is small, even for large rain showers. A large amount of the precipitation is stored on the surface of the riparian area. At about 25% of the riparian area, water is continually stored on the surface (depression storage). This water forms a large amount of the "direct" runoff. Measurements of isotope tracers (silica and deuterium) suggest that subsurface water forms the largest amount of the discharge. The deeper groundwater, however, also contributes to the quick discharge, caused by processes as piston flow and

groundwater ridging. All these processes together play a role in the generation of runoff and make it difficult to conceptualise the runoff generation processes in the riparian area.

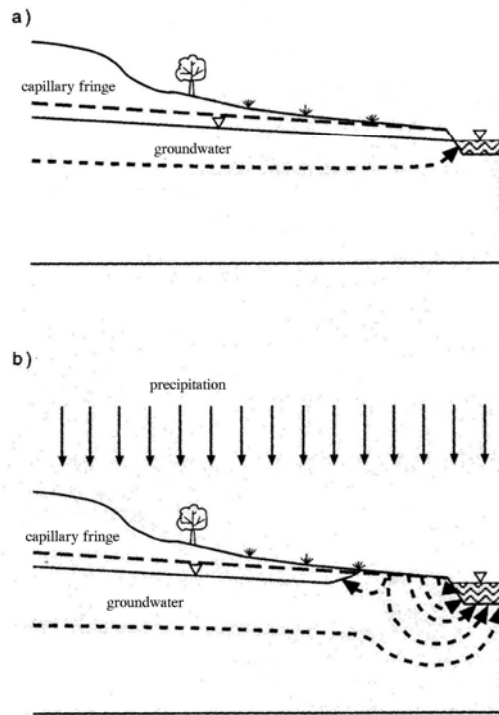


**Figure 2.6 Rising water table caused by groundwater ridging. a) situation before precipitation, b) development of a groundwater ridge (Uhlenbrook & Leibundgut, 1997)**

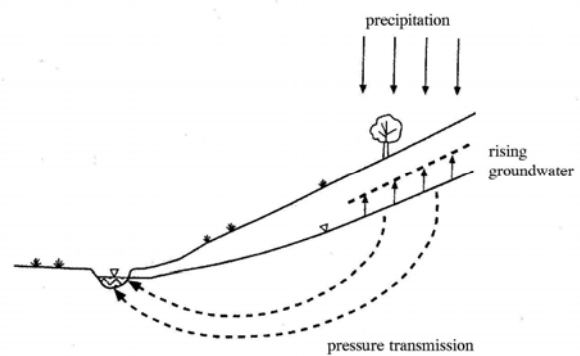


**Figure 2.7 Rising water table caused by piston-flow (Uhlenbrook & Leibundgut, 1997)**

### 3. Methods

In this chapter the original TAC-D model is described and the programming language, PCRaster, used in TAC-D is explained. The last paragraph of this chapter elaborates silica as a geological tracer.

#### 3.1. Description of the dynamic GIS-program PCRaster

##### 3.1.1. Basic concept

PCRaster is a Geographical Information System (GIS). The raster-based program is developed in the early 1990s at the University of Utrecht. The Dynamic Modelling Language, which is included in PCRaster, is a computer language developed for environmental modelling. About 120 different functions are available, which can be used in combination with mathematical notations (like *if then, else*). The main advantages of the Dynamic Modelling language are:

- no specialist programming knowledge is required; all that is necessary, is a familiarity with mathematical notations. Therefore, a model can easily be developed or adapted.
- the language is embedded in the PCRaster GIS, so data exchange between model and GIS is unnecessary. Furthermore, spatial-temporal data can be used or stored at any time during a model run. (Van Deursen, 1995a)

It is also possible to develop own functions written in Delphi or C++. Roser *et al.* (2001) has developed two external functions for the soil routine (Ch. 3.2.6) in TAC-D.

The central concept of PCRaster is a discretization of a catchment in space, resulting in cells of information. Each cell can be regarded as a set of attributes that represents the catchment characteristics for that area. The cell can receive and transport information from and to other cells. This representation of the catchment is often referred to as 2.5 D. The lateral directions in a landscape are represented by a set of neighbouring cells making up a map. The relations in vertical directions, for instance, between soil layers, are simulated by storing attributes for different map layers in a cell, see Figure 3.1. (PCRaster Research Team, unknown year)

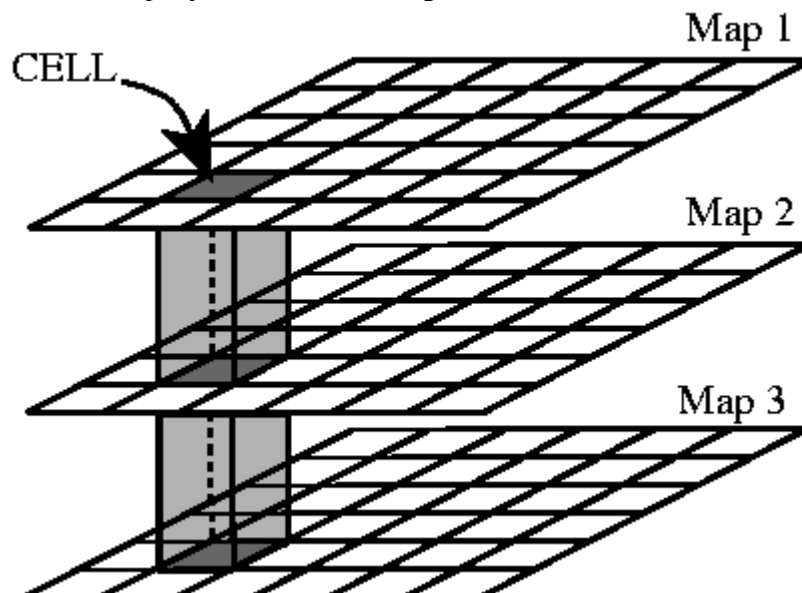


**Figure 3.1** Different attribute values of one cell stored in three map layers (PCRaster Research Team, unknown year)

The Dynamic Modelling language is integrated in the GIS at a high level (Figure 3.2). Therefore, data exchange problems do not exist, because the database of the GIS is the

database of the model and vice versa. Below, an overview of the advantages and disadvantages of high level integration is presented.

**Advantages of high level integration:**

- integration of GIS functionality for manipulation of input, results and formulation of the models;
- no overhead for conversion between GIS and models and between individual models
- rapid development of new models, and
- easy maintenance of models.

**Disadvantages of high level integration:**

- current generation of commercial GIS packages (e.g. ArcInfo) does not fully support dynamic modelling;
- investment in development of tools and functionality is high, and
- lack of expert insight may yield invalid model concepts and formulations; the user is fully responsible for the model formulation (Van Deursen, 1995b).

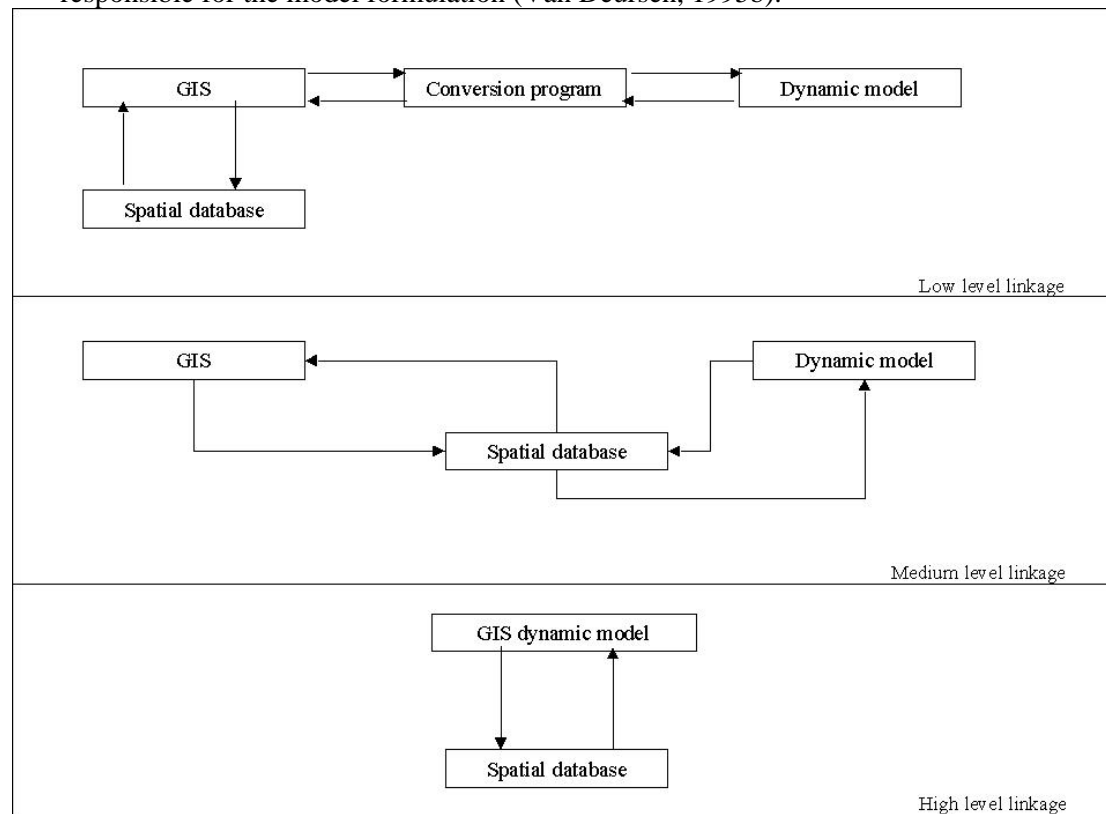


**Figure 3.2 Different levels of linkage between model and database (Van Deursen, 1995b)**

### 3.1.2. Structure of Dynamic Modelling

Multiple sorts of data are used in PCRaster. Six different sorts of data type<sup>1</sup> can be defined per map. For;

- data in classes: boolean, nominal and ordinal data types;
- data on a scale: scalar data type;
- data on a circular scale: directional data type;
- a local drain direction network: ldd data type.

Relations between PCRaster maps can be defined by tables. By using such a table, a new map with new characteristics can be created. In Dynamic Modelling time series are linked to a PCRaster map to control spatial data that vary over time and space. This means that for each time step a different spatial data set can be imported or stored. The last kind of data used, is

<sup>1</sup> the specific PCRaster terminology is underlined in this paragraph



point data column files. Point data consist of a x,y-coordinate and one or more attribute values, mostly gathered through field study. For example, precipitation measured at a meteorological station and runoff measured at a gauging station are typical point data.

In the Dynamic Modelling language, the model is divided into sections. PCRaster defines 5 sections: i.e. Binding, Areamap, Timer, Initial and Dynamic.

The binding section defines the different names in the code; it binds the database file names to the names of a variable in the model. The areamap section defines the model area and the modelling resolution. This is done by specifying a clone map. All maps produced or used by the model have the location attributes of the clone map. The timer section specifies the duration of a model run (start and end time) and it specifies the time slice of the timestep (dt). In the initial section, all the initial attribute values, needed for the start of the dynamic section, are set. The dynamic section defines for each timestep the operations that result in the (map) output for that timestep. This concept is presented in Figure 3.3.

The programming is done in Proton computer language, which can be run through PCRaster Shell (MSDOS).

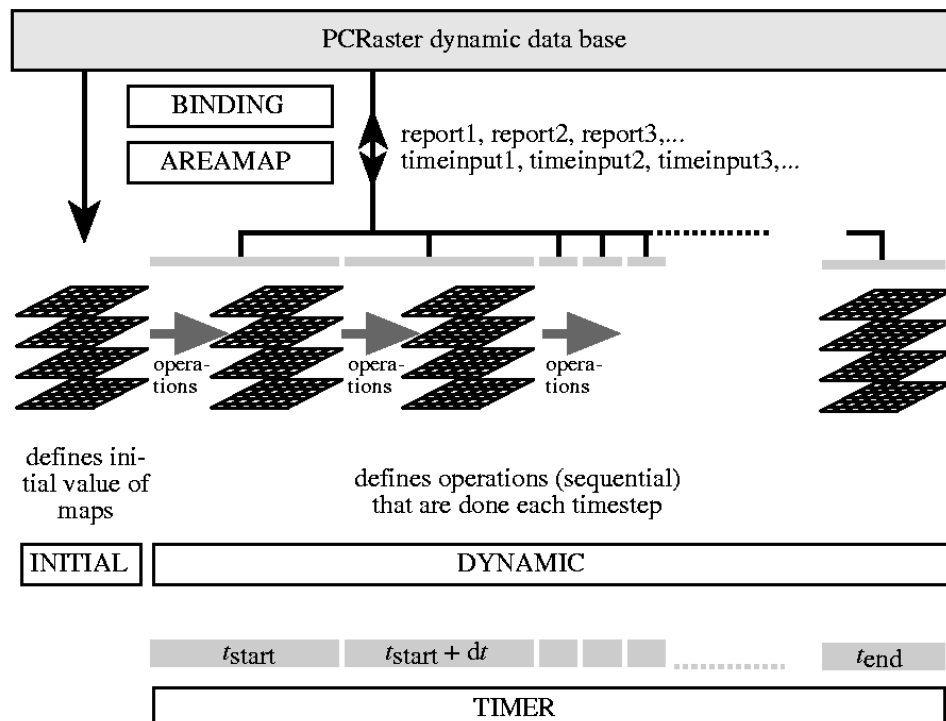


**Figure 3.3** Schematic representation of a dynamic model (PCRaster Research Team, unknown year)

## 3.2. Description of the model TAC-D

### 3.2.1. Introduction

TAC-D was developed as an extension to the already existing semi-distributed, process-oriented catchment model TAC (Tracer Aided Catchment model). To improve the conceptual modelling approach, the TAC model was integrated in a dynamic geographical information system (Ch. 3.1). The conceptual TAC model simulates hydrological processes through different reservoir concepts for zones with the same dominating runoff generation processes. The limitations of the former TAC model were mainly caused by the restricted spatial and temporal resolution. The semi-distributed concept of the TAC model ignored the spatial position and the lateral exchange between single runoff generation areas (cells). To realise an adequate spatial discretization in TAC, the model was integrated in the GIS-raster based

program PCRaster. The newly developed model was called TAC-D (Distributed Tracer Aided Catchment model).

TAC-D consists of different modules: a Snow routine, a Soil routine, a Runoff generation module and a Riparian area module. In this chapter, first the general model concept of boxes and the flow patterns between these boxes is described. After that, the different modules are explained. This subchapter is based on Roser *et al.* (2001), who developed TAC-D.

### 3.2.2. Model outlook

The model is based on the water balance for a certain time step:

$$S(t) = S(t-1) + P + Q_{in} - ET_a - Q_{out} \quad \text{Equation 3.1}$$

With:

- $S(t)$  = storage at time  $t$  [ $\text{m}^3$ ]
- $S(t-1)$  = storage at time  $t-1$  [ $\text{m}^3$ ]
- $P$  = precipitation [ $\text{m}^3$ ]
- $Q_{in}$  = lateral inflow in storage [ $\text{m}^3$ ]
- $ET_a$  = actual evaporation from storage [ $\text{m}^3$ ]
- $Q_{out}$  = lateral inflow out of storage [ $\text{m}^3$ ]

TAC-D is organised in different boxes, with defined storages, each representing a different runoff generation zone. Each box has more or less the same layout (see Figure 3.4). The water balance (Eq. 3.1) is solved for each box. The quantities in TAC-D are presented in mm, this can be done because the cell area is constant for each cell.

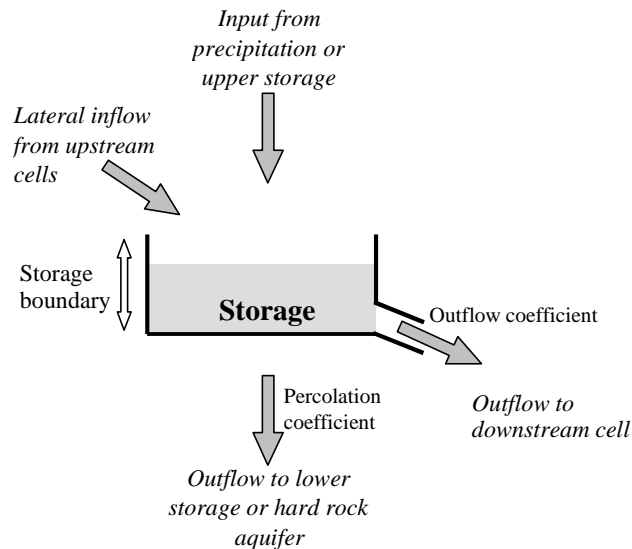


**Figure 3.4 General storage concept of TAC-D (after Roser *et al.*, 2001)**

The storage concept is based on the formula:  $Q(t) = k \cdot S(t)$  **Equation 3.2**

- With  $Q(t)$ : outflow [ $\text{mm/h}$ ]
- $k$ : outflow coefficient (hydraulic conductivity) [ $\text{h}^{-1}$ ]
- $S(t)$ : storage capacity [ $\text{mm}$ ]

The input consists of precipitation or percolation from the upper box. The percolation from the box shown in Figure 3.4 is the amount of water transported to a lower box, or in the case of a lower box, the amount of water to the groundwater in the hard rock aquifer. The outflow parameter transports the water from the storage (minus the water what percolates to a lower box) to a downstream cell. The last box in the cascade is the stream. In the stream, the kinematic wave equation is used to calculate the discharge at the outlet.

In TAC-D three different types of storage boxes are defined:

- Upper Storage box (*sUS\_box*);
- Lower Storage box (*sLS\_box*), and
- Micro Topographic Depression box (*sMTD\_box*).

The *sUS\_box* has as input water that comes from the soil routine (Ch. 3.2.6), the *sLS\_box* gets water from percolation from the *sUS\_box*, and the *sMTD\_box* has precipitation as input. All outflows are defined as variables  $sQ_{...}$  (Eq. 3.2), with  $sQ_{US}$  for the upper storage,  $sQ_{LS}$  for the lower storage, and  $sQ_{SOF}$  (SOF meaning Saturated Overland Flow) for the *sMTD\_box*. The hydraulic conductivity of each box (Eq.3.2) is named  $..._K$ , i.e.  $cUS_K$  for the upper storage,  $cLS_K$  for the lower storage and  $cMTD_K$  for the micro topographic depression. The storage boundary is defined by the parameters  $cUS_H$ ,  $cLS_H$  and  $cMTD$ . The leakage to lower storages is defined by  $cUS_T$  for the percolation from upper to lower storage and  $cAll_P$  for the percolation to the hard rock aquifer. The variable  $cAll_P$  is the same for every runoff generation zone, because of the assumption that the connection to the hard rock is similar for each runoff generation zone.

When the lower storage is full, the excess water is routed to the upper storage. The *sMTD\_box* has a limited storage capacity, to approach the saturated field conditions, and therefore has an overflow possibility. The water that flows over the storage boundary is added to  $sQ_{SOF}$ .

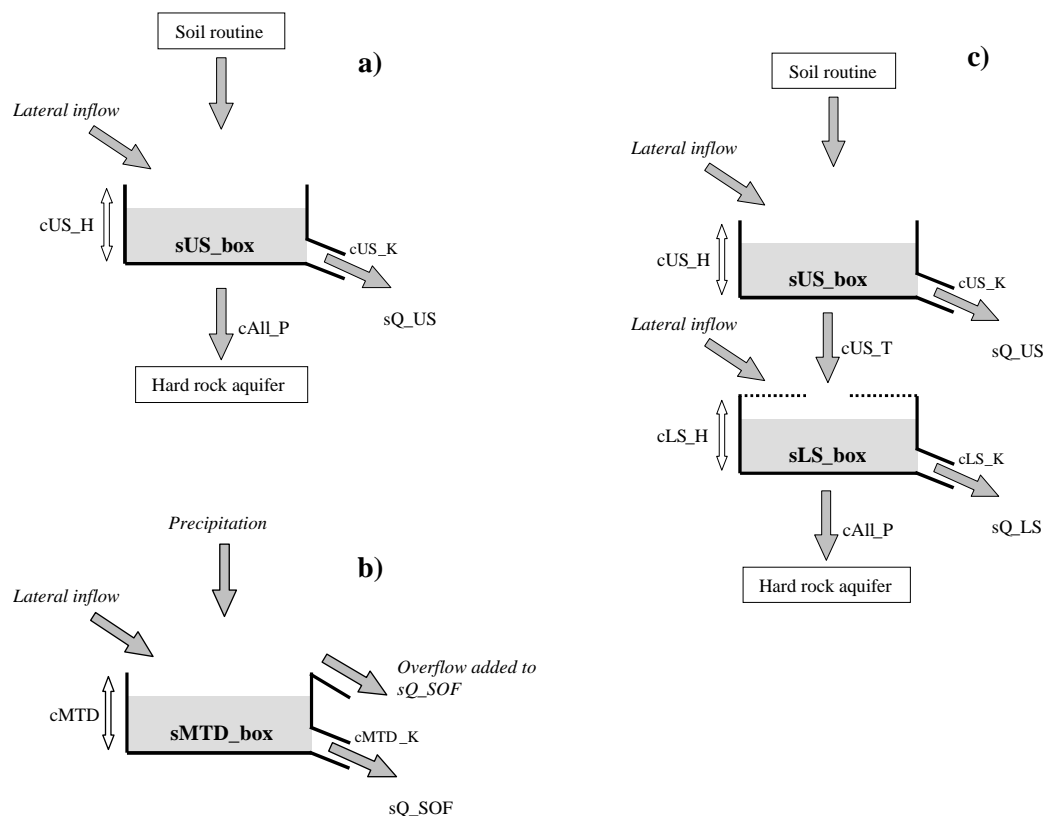


**Figure 3.5 Different storage concepts used in TAC-D (after Roser *et al.*, 2001)**

### 3.2.3. Local drain direction network

To determine the cascade of cells (position of certain cell relative to upstream cells) a local drain direction network (ldd) is defined. In PCRaster, it is possible to compile a ldd using the digital elevation model (dem). The flow direction from one cell to another is determined by the steepest slope. Cells with infiltration (sinks) or exfiltration (sources) are called pits. To prevent that the actual stream flows on a different location than were the ldd simulates the stream, the dem is manipulated. The stream is predefined in the dem by giving it an artificial

low elevation. In this way, the ldd is forced to follow the stream (Figure 3.6). The outlet of the catchment is also defined as a pit-cell.

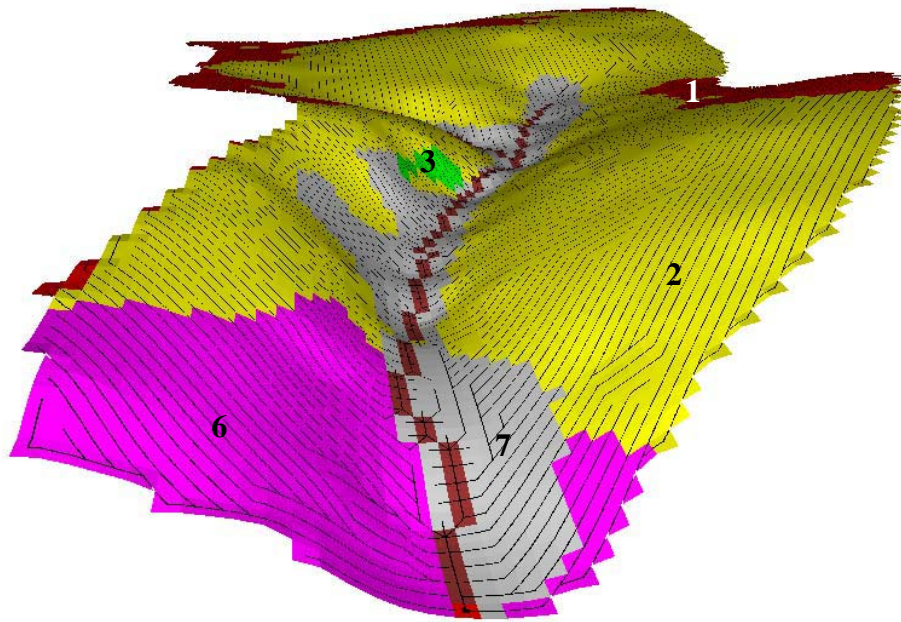


**Figure 3.6 Haldenbach micro-catchment in 3D, with the different runoff generation zones (numbers explained in Ch. 3.2.7), the stream and the ldd**

#### 3.2.4. Lateral flows

The difference between the old TAC and the newly developed TAC-D is the spatial discretization. The runoff follows the local drain direction (ldd) network. Every cell represents one box per map layer (Figure 3.1), which is connected to the other boxes through the ldd. This can be visualised through a cascade of barrels (Figure 3.7). When the slope is long, the cascade becomes longer, which represents the time lag between the precipitation event and the moment when the water reaches the stream. This means that the outflow coefficient  $k$  (Eq. 3.2) is negatively correlated to the length of the cell. A water particle has to go through more cells when the cell length is smaller, so the time the particle stays in one cell has to be smaller, compared to the time needed to go through less, bigger cells. Therefore, the outflow coefficient is scale dependent.

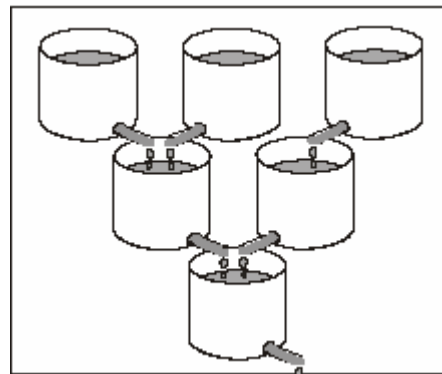


**Figure 3.7 Cascade of barrels**

#### 3.2.5. Snow routine

In the snow routine, precipitation is simulated as snow when the temperature drops under a certain threshold temperature. The snow melts when the air temperature exceeds that threshold temperature. The amount of water in the snow is calculated with use of a water holding capacity parameter. The snow absorbs the melt water until this water holding capacity is reached. The remaining water is routed to the soil routine.

### 3.2.6. Soil routine

The soil routine in TAC-D is used to calculate the amount of accumulated soil moisture for each runoff generation zone except for the riparian area. As input for the soil routine the water from the precipitation, or in case of snow, the water from the snow routine, is used. From the amount of soil moisture is determined, how much water is stored in the unsaturated zone and how much water is routed to the runoff generation module (Ch.3.2.7). The actual evaporation is also related to the amount of soil moisture (Ch. 3.2.11).

### 3.2.7. Runoff generation module

In the TAC-D model for the Brugga catchment different runoff generation zones were defined (Figure 3.8):

#### 1. Flat hilltops (slope 0-6°)

Flat hilltops consist of a Tertiary weathering layer on hard rock. The water in the weathering zone has long residence times. The flat hilltops are conceptualised by one box. (Figure 3.5a)

#### 2. Periglacial drift cover (layered) (slope 6-25°)

The runoff dynamics of the periglacial drift cover is dominated through the layered zone (Figure 2.5). The hydraulic permeability decreases with depth. This is conceptualised by 2 boxes (Figure 3.5b), one for the runoff defined by the macropores and one box with slow runoff dynamics, representing the less permeable base layer. The percolation from the upper into the lower box is very small, caused by the slumped base layer.

#### 3. Not-layered drift cover on the main layer (slope 25-34°)

The not-layered drift cover is conceptualised by 2 boxes (Figure 3.5b). The box of the main layer is the slower reacting box, the other box (representing the cover layer) has high runoff dynamics, caused by the flow through the macropores. The percolation between the box representing the drift cover and the box representing the main layer is relatively small. The main layer has a limited storage capacity, because the layer is not very thick, caused by the slope. The lateral flow will first fill the lower box, when this is full the water is routed to the upper box (Ch. 3.2.2).

#### 4. Boulder field (>34°)

The boulders in a boulder field can be very large and the hydraulic conductivity is therefore very high. This quick response is conceptualised by one box with a high outflow constant (Figure 3.5a). This type of geology is not present in the Haldenbach micro-catchment and was therefore not discussed in Chapter 2.

#### 5. Accumulation zone at foothills (slope 0-25°)

The foothills are the areas near the stream, consisting of alternating sediment layers, mostly originated from Holocene age. The stratified sediments have a good permeability but the fine-grained layers in between have a moderate permeability. These alternating layers are approached by using 2 boxes (Figure 3.5b). The upper box represents both the good permeable sediment layers and layers dominated by macropore flow. The lower box conceptualises the moderate permeable fine-grained (loamy) layers. This box has a limited storage capacity, the rest of the water is routed to the upper box. So this water is quicker distributed.

#### 6. Moraine area

It is difficult to define the characteristics of the moraine area, because of the large differences in thickness and composition. In general, it is assumed that the moraines have a moderate

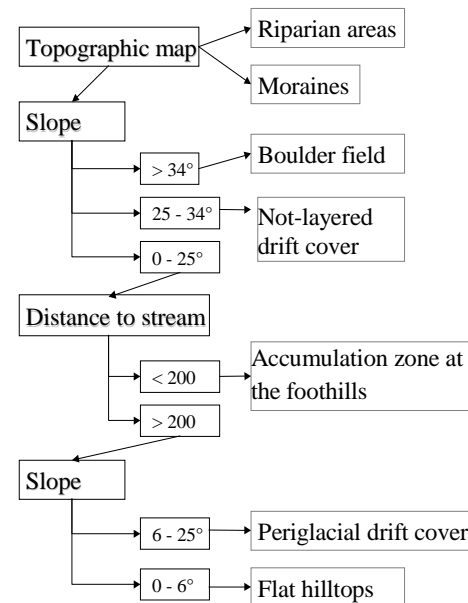


**Figure 3.8 Assignment scheme for runoff generation zones (after Roser, 2001)**

hydraulic conductivity and slow runoff processes are typical for the area. This behaviour is conceptualised by one box (Figure 3.5a).

## 7. Riparian area

The riparian area is located close to the stream and is (nearly) saturated during the whole year. A quick discharge can be generated because of the near-stream location. When the surface storages are filled, additional precipitation can cause an increase in the discharge almost without a time lag. This is conceptualised into the model by defining one box, with a limited storage capacity, when this capacity is reached, the water is directed into the stream. The normal outflow of the box is delayed. The precipitation is not lead through the soil routine (as done by the other runoff generation zones), and the evapotranspiration is potential, because the riparian area is assumed to be saturated throughout the whole year (Figure 3.5c).

## Hard rock aquifer

One box with a very slow response time represents the water storage and flow in the hard rock aquifer (Figure 3.9). This runoff is mainly responsible for the base flow. All the above mentioned runoff generation zones, except the riparian area, recharge the deep groundwater in the hard rock aquifer. This happens by percolation from the lower box, or in case of only one box, percolation from the upper box (Figure 3.5a and 3.5b). The outflow of the deep groundwater box is directly into the stream. So, deep groundwater is assumed not to feed the riparian areas in this concept.

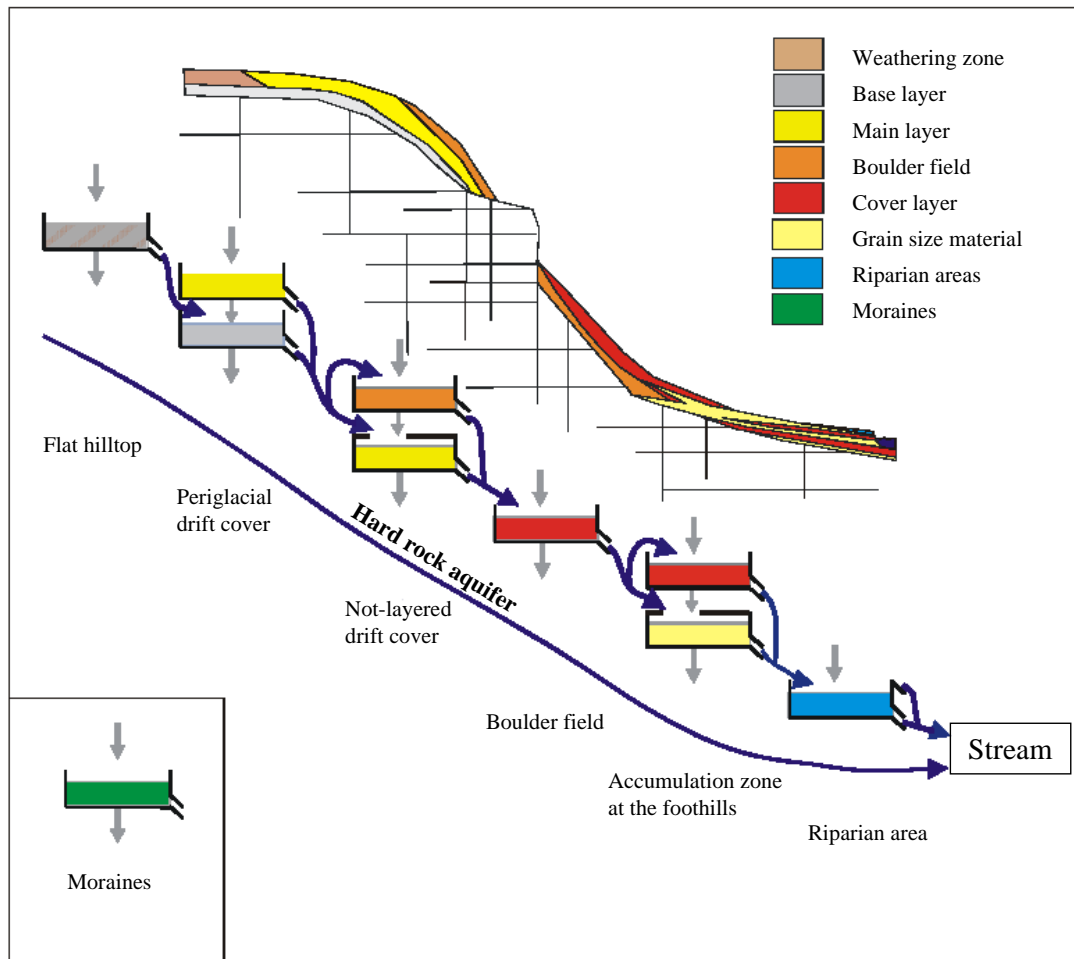


**Figure 3.9** Storage concept of the different runoff generation zones in TAC-D (after Roser *et al.*, 2001)

### 3.2.8. Stream cells

By integrating stream cells into the raster (Ch. 3.2.3), the stream becomes too wide. For instance, in the Haldenbach micro-catchment the cells are only 5 by 5 m. This would mean, however, that the stream is 5 m wide, while in reality the maximum width is 0.6 m. To overcome this problem, the stream cells have 2 functions. The cell is defined both as a runoff generation zone (Ch. 3.2.7) and as stream cell. The concept is explained in Figure 3.10. Figure 3.10a explains the horizontal plain and Figure 3.10b the 2 map layers. The upper layer consists of a row of stream cells, where only the shaded part is assigned as water for the stream. The area of the shaded part is calculated from the width of the stream on the cell length. The remaining water flows through the stream cell to the runoff generation zone.

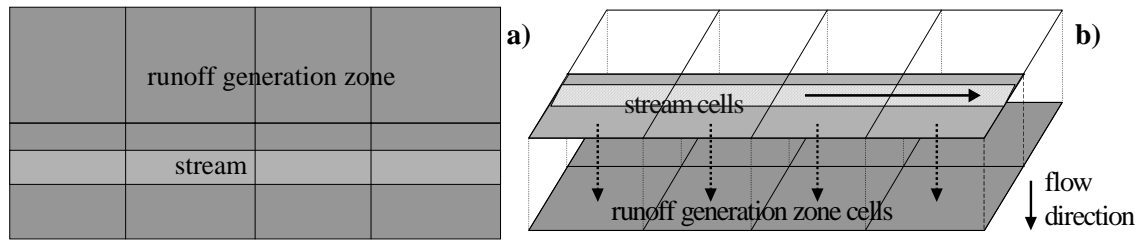


**Figure 3.10 Concept of the stream cells; in Figure 3.10a the horizontal plane displayed, in Figure 3.10b the layered concept in TAC-D is presented**

### 3.2.9. Urban areas

Water falling on urban areas or paved roads is directly transported to a downstream cell through the ldd. An urban area cell is divided into a sealed area and a non-sealed area. The part that is sealed generates the direct discharge, the remaining water goes through the soil routine.

### 3.2.10. Wave building

A flood wave in a stream is transformed (delayed and smoothed) during transport in a stream (Torfs, 2001). To simulate this transformation, the kinematic wave equation is used. This function of PCRaster is based on the continuum equation, the equation of preservation of mass and the Manning-Strickler equation. In TAC-D the transformation of the wave is calculated in shorter timesteps than used for the other processes in the model (steps smaller than one hour). The length of the timesteps used to calculate the wave building is dependent on the cell area. The kinematic wave equation is among other things used to calculate the discharge at the outlet of the micro-catchment.

### 3.2.11. Climatic input data

The only time dependant data that are used as input in TAC-D are climatic data. The different climatic data will be described below.

#### *Precipitation*

Precipitation measurements may have a systematic error, caused by wind-effects. In TAC-D, this is corrected through the following equation:

$$P_{cor} = P_{measured} \cdot (a + b \cdot u_w) \quad \text{Equation 3.3}$$

With  $P_{cor}$  = corrected precipitation [mm/h]  
 $P_{measured}$  = measured precipitation [mm/h]  
 $u_w$  = wind velocity [m/s]  
 $a, b$  = correction factors [-],[s/m]

In this study the corrected precipitation, measured at one station was extrapolated to the entire area through a combination of Inverse Distance Weighing (IDW) and an elevation factor. The

elevation factor was calculated from a regression equation based on the long-term precipitation from measurement stations at different altitude.

#### *Air temperature*

The air temperature in a particular cell is dependent on the elevation, and it is therefore interpolated from the measured temperature at a particular station, by means of an elevation-dependent regression.

#### *Global radiation*

To determine the potential evaporation the global radiation has to be known. The global radiation is calculated in the program POTRAD5 (Potential Radiation Equator model<sup>(c)</sup>) which uses the relative sunshine as input (Van Dam, 2000).

#### *Potential evapotranspiration*

The potential evapotranspiration is calculated with the ETP-module developed by Ott *et al.* (2002) in PCRaster, which is based on the equation of Penman-Monteith (Equation 3.4) (Allen *et al.*, 1998).

$$ET_p = \frac{1}{\lambda} \frac{3.6 \cdot \frac{\Delta}{\gamma} \cdot (R_N - G) + \frac{\rho \cdot c_p}{\gamma \cdot r_a} (e_s - e_a) \cdot t_i}{\frac{\Delta}{\gamma} + 1 + \frac{r_s}{r_a}} \quad \text{Equation 3.4}$$

With:  $ET_p$  = potential evaporation [mm]  
 $\lambda$  = latent heat ( $\lambda = (2500.8 - 2.372 \cdot T)$  kJ/kg, with  $T$  = temperature [°C])  
 $\Delta$  = slope of the saturation vapour pressure temperature relationship [kJ/kg]  
 $\gamma$  = psychrometric constant [hPa/K]  
 $R_N$  = net radiation [Wh/m<sup>2</sup>] (1 Wh/m<sup>2</sup> = 3.6 kJ/m<sup>2</sup>)  
 $G$  = soil heat flux [Wh/m<sup>2</sup>]  
 $\rho$  = mean air density at constant pressure [kg/m<sup>3</sup>]  
 $c_p$  = specific heat capacity of air [kJ/kg·K]  
 $e_s$  = saturation vapour pressure [kJ/kg·K]  
 $e_a$  = actual vapour pressure [kJ/kg·K]  
 $t_i$  = time of interval [s]  
 $r_a$  = aerodynamic resistance [s/m]  
 $r_s$  = surface resistance [s/m]

Contrary to the Turc-Wendling equation used in an earlier version of TAC-D, in Eq. 3.4 the land use plays an important role in the calculation of the evapotranspiration, through the addition of plant physiologic characteristics ( $r_s$ ). More detailed information about the calculation of the potential evaporation with Penman-Monteith can be found in Ott *et al.* (2002).

#### *Actual evapotranspiration*

The calculation of the actual evapotranspiration from the potential evaporation is done within TAC-D. In the soil routine (Ch. 3.2.6), the actual soil moisture storage is used to determine the actual evapotranspiration from all runoff generation zones, except for the riparian area. The evaporation from the riparian area is supposed to be potential, because of the assumption that the riparian area is saturated during the whole year. The evaporation of the snow cover, if present, is added to the actual evaporation.

#### 3.2.12. Flow chart of the TAC-D model

To give an overview of all modules in TAC-D a flow chart was made (Figure 3.11).



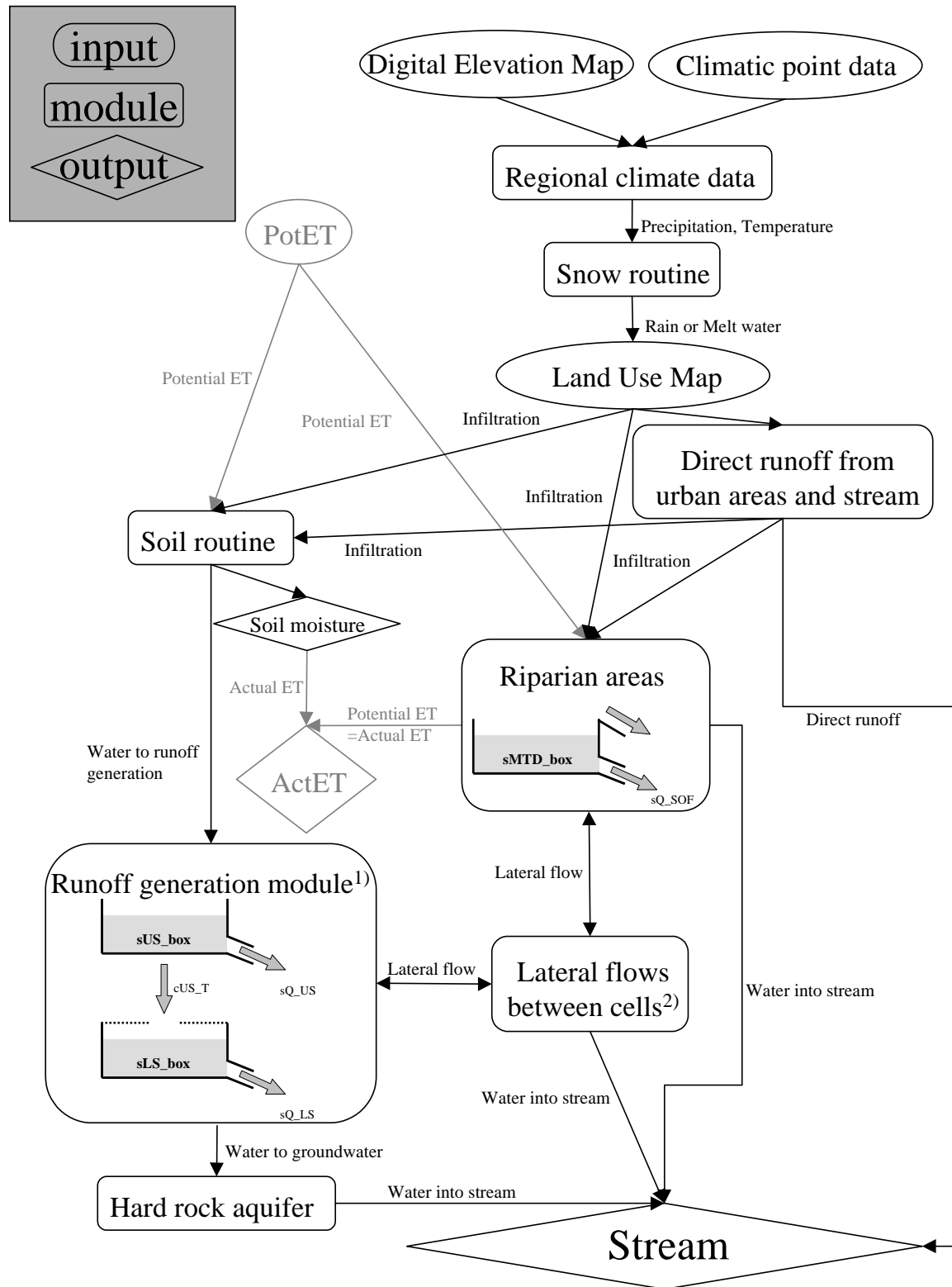


**Figure 3.11 Flow diagram of TAC-D¹; legend in the grey box <sup>2</sup>**

<sup>1</sup> Not all runoff generation zones have a lower box (Ch 3.2.7)

<sup>2</sup> This box represents water flowing from runoff generation cells to riparian areas and vice versa

### 3.3. Silica as a geological tracer

#### 3.3.1. Introduction to Silica

Silica is a geological tracer, this means that the silica concentration in the water indicates through which geological formation the water has flowed. Dissolved silica has been used as a useful tracer for tracing hydrological flow paths, because of its presence in groundwater and stream water from the weathering of silica rocks and its near-zero concentration in precipitation (Uhlenbrook, 1999).

In an aquatic environment dissolved silica is present as silicic-acid ( $\text{H}_4\text{SiO}_4$ ). This is a weak acid and therefore it has a low weathering potential. The degree of weathering is dependent on the temperature, pH and the contact time of the water with the hard rock. By a high temperature, a low pH and a long contact time the weathering is maximal. Water in the deeper geological formations is assumed to have higher silica concentrations due to the longer residence times and the higher amount of weatherable minerals.

Most of the dissolved silica originated from Na-feldspar, Ca-feldspar, olivine and amphibole (hornblende), because these are easy weatherable minerals (Figure 3.12 and Sieder *et al.*, 2000)

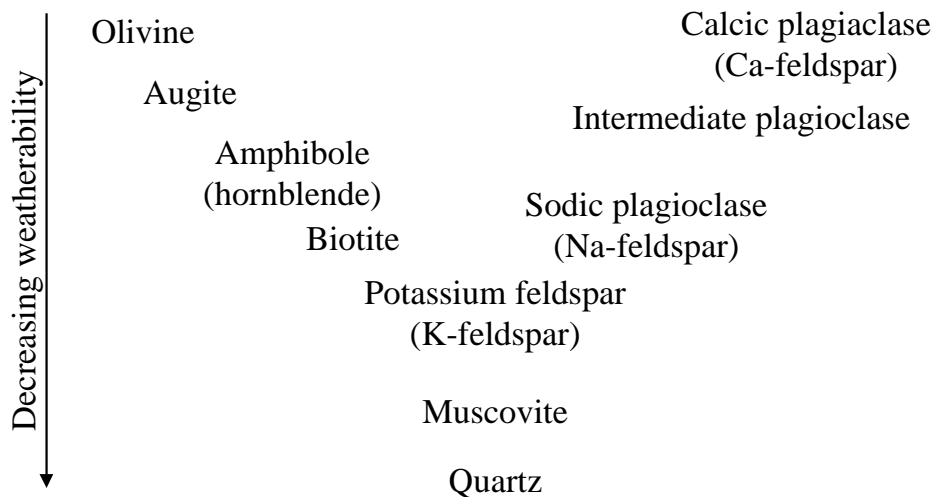


**Figure 3.12 Goldich weathering sequence (Goldich *fide* Appelo & Postma, 1999)**

#### 3.3.2. Silica concentrations in the Brugga catchment

Water samples from the Brugga catchment area show different silica concentrations for water that followed different flow paths. Three main flow systems were defined in a research by Uhlenbrook (1999).

1. *Direct runoff* coming from the riparian areas, the urban areas and from the boulder fields. The direct runoff consists of precipitation and water from shallow subsurface flow. This water can contribute up to 50% of the total runoff, shortly after the shower. For longer periods (years) its share is about 10%.
2. *Flow-system-2* consists of water from the periglacial drift cover, with a residence time of 2-3 years.
3. *Flow-system-1* with water from the weathering zones of the flat hilltops and the hard rock aquifer. The mean residence time is 6-9 years. This water contributes to ca. 20% of the total runoff.

After identification of water from the different flow systems, the silica concentrations were determined (Table 3.1).

**Table 3.1 Characteristics of the different flow systems (Uhlenbrook, 1999)**

<b>Flow system</b>	<b>residence time</b>	<b>Si concentration [mg/l]</b>	<b>runoff-dynamics</b>
<i>Direct runoff</i>	hours-few days	0.3	high
<i>Flow-system-2</i>	2-3 years	4.2	medium
<i>Flow-system-1</i>	6-9 years	6.0	low

As can be seen from Table 3.1, there is a clear relation between the residence times and the measured concentrations. The longer the residence time, the higher the concentration silica in the water.

## 4. Input data and maps for applying TAC-D to the Haldenbach micro-catchment

This chapter describes all input data and the maps that were created to run TAC-D for the Haldenbach micro-catchment. The time discretization of the model can also be found in this chapter. Finally, model performance criteria are discussed here.

### 4.1. Existing data

Almost all measurements used in this study were done in the autumn of 1999 (Sieder *et al.*, 2000). During the research in the Haldenbach micro-catchment, also the different ions in the water from the gauging stations and from the precipitation were measured. In this study, only the data on silica was used. The climate data were obtained from the meteorological station at Schauinsland (temperature, humidity, wind speed and additional rain data) and the station at Feldberg (sunshine duration data). The location of Schauinsland and Feldberg can be found in Figure 2.1.

### 4.2. Pre-processing of the spatial data

#### 4.2.1. Digital Elevation Model

To compile a digital elevation model (dem) of the Haldenbach micro-catchment a topographic map was used. From the tk50 (topographic map, scale 1: 50.000) the contour lines were digitalized in ArcView and converted to a dem in ArcInfo. For this micro-catchment, a raster of 5 by 5 m was used. Subsequently, a local drain direction network (ldd) was compiled using this dem within PCRaster.

The conversion of co-ordinates to a raster of 5 by 5 m slightly changed the area of the micro-catchment. An overview of increase of the area is given in Table 4.1. The new area is used in all calculations made with TAC-D.

**Table 4.1 Changed area caused by digitalizing the micro-catchment**

cell length	Catchment					
	MU			OM		
	actual area [m <sup>2</sup> ]	no. of cells [-]	total area of all cells [m <sup>2</sup> ]	actual area [m <sup>2</sup> ]	no. of cells [-]	total area of all cells [m <sup>2</sup> ]
5 m	208.000	8709	217.725 (5%)	181.000	7616	190.400 (5%)

#### 4.2.2. Map of zones with dominant runoff generation processes

The different zones were determined from the description mentioned in paragraph 3.2.7. The riparian area was digitalized from the tk50 map (Figure 2.2) and the map made by Sieder *et al.* (2000) in ArcView. The moraines were digitalized from a geological map. The other areas were defined by their slope and distance to the stream (Figure 3.8). From all runoff generation zones defined in the Brugga catchment (Ch. 3.2.7) only the boulder field (4) and the accumulation zone at the foot hill (5) are not present in the Haldenbach micro-catchment. The map in Figure 4.1 shows the different runoff generation zones.

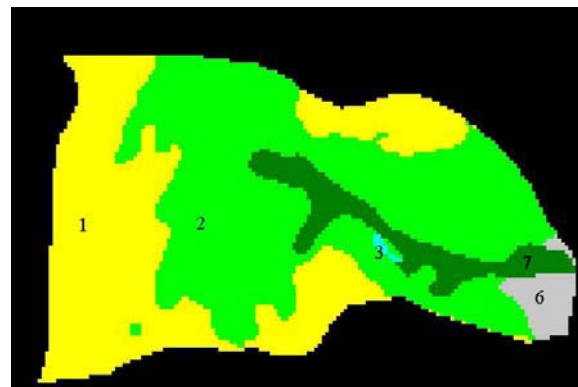


**Figure 4.1 Runoff generation zones in the Haldenbach catchment (1: flat hilltops, 2: periglacial drift cover, 3: not-layered drift cover, 6: moraines, and 7: riparian area)**

#### 4.2.3. Other maps

Other maps that were compiled to run TAC-D are a map with:

- urban areas, derived from the topographic map;
- the location of the stream, also derived from the topographic map;
- the cross section of the stream;
- the Manning coefficient of the stream;
- the location of the gauging station;
- the location of the meteorological data, and a
- clone map, to be sure that all maps are equal and fit over each other.

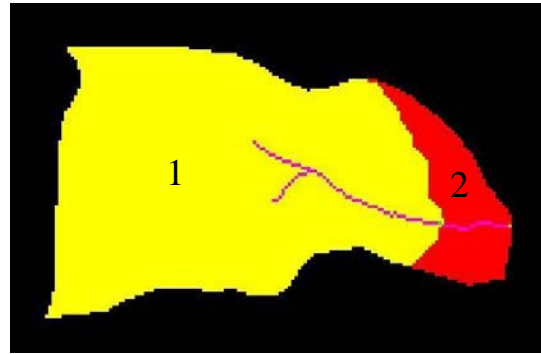


**Figure 4.2 Sub-catchments of the Haldenbach micro-catchment (1: OM, 2: MU-OM, 1+2: MU)**

Figure 4.2 shows an example of a compiled map consisting of three different map layers representing the Haldenbach micro-catchment, the Haldenbach (stream) and the two sub-catchments (OM and MU).

### 4.3. Pre-processing of the non-spatial data

TAC-D uses timesteps of 1 hour, except for the kinematic wave module (Ch. 3.2.11). Therefore, all non-spatial data were converted to 1-hour data. There were data available for the Haldenbach micro-catchment from the observation period 23 October – 6 November 1999.

#### 4.3.1. Rain data

The rain was measured at 2 stations; i.e. a rain gauge in the Haldenbach micro-catchment (Sieder *et al.*, 2000) and a gauge at the station of the German Wetter Services (DWD) located in Schauinsland. The data from Schauinsland is measured every half hour and the data from the Haldenbach was obtained every 10 minutes. These data were transformed to hourly data. Eventually, only one station was defined in the model to restrict calculation time. Therefore, only the data obtained in the Haldenbach micro-catchment was used. The data from the Schauinsland station was only used to check the Haldenbach data on errors. Equation 3.3 was used to correct the rain on measuring errors caused by wind. For the Haldenbach micro-catchment, the elevation factor from the Brugga catchment (Roser *et al.*, 2001) was used. This all resulted in an elevation-dependent precipitation per timestep.

During the observation period from 23 October to 6 November 1999, 6 rain showers occurred (Figure 4.3). The first and third shower were very small (1-2 mm). The second and fifth showers were large (ca. 60 mm) with a long duration. More detailed information can be found in Annex B.

#### 4.3.2. Discharge

During the measurements in October and November 1999, 2 V-weirs were used to measure the discharge (Figure 4.3). Gauging station MU (lower gauging station) only worked until 28 October 1999. After 7 November, no data is available, because of snow accumulation on the micro-catchment.

The small showers (no. 1 and 3) had hardly any effect on the discharge. The large showers, however, produced a peak-discharge of about 0.02 m<sup>3</sup>/s. The base discharge is about 0.003 m<sup>3</sup>/s. After a rain shower, the base runoff becomes slightly higher. Figure 4.3 shows that the micro-catchment reacts very quickly on precipitation, as mentioned in Ch. 2.3.3. The saturated riparian area is responsible for this quick reaction.

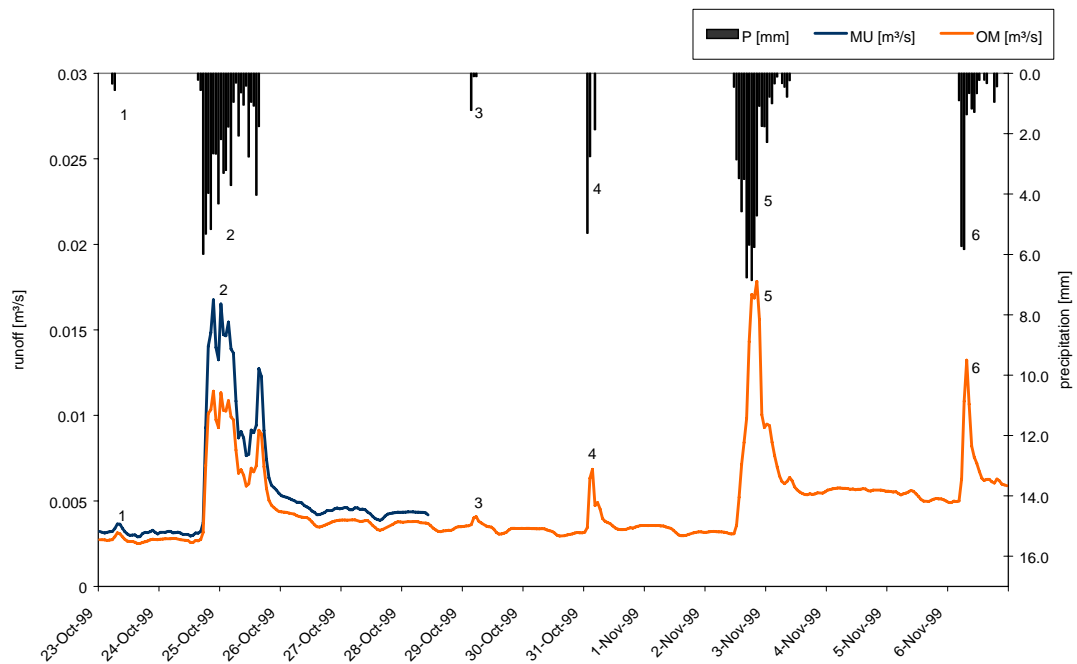


**Figure 4.3 Precipitation (right y-axis) and runoff (left y-axis) in the Haldenbach micro-catchment**

#### 4.3.3. Air temperature

In the TAC-D model, the observed air temperature at a meteorological station was modified for a certain cell by an elevation-dependent regression equation to simulate the effect of inversion layers, which are common in mountainous areas. This correction is not applied to the Haldenbach micro-catchment, because the meteorological station Schauinsland is not far away and had a similar altitude. Furthermore, the differences in height in the micro-catchment are negligible (Annex A). Therefore, it is assumed that a correction for inversion is not needed.

#### 4.3.4. Sunshine duration

The relative sunshine duration (-) was obtained from the DWD station Feldberg (Figure 2.1). This is the only station available, therefore it was assumed that the sunshine duration is the same for the Haldenbach micro-catchment. This assumption makes it possible to define a meteorological station in the catchment itself. This has as a benefit that the area the model has to go through in the calculation is smaller. Normally, PCRaster creates cells between the different gauging stations for the calculation. Therefore, when the gauging station is inside the micro-catchment instead of kilometres away, less cells have to be go through in the operation and this shortens the calculation time.

#### 4.3.5. Wind speed and humidity

The wind data was obtained from meteorological stations Schauinsland and St. Wilhelm. For periods that data from Station Schauinsland was lacking, a regression equation obtained from these two data sets was used fill in data gaps. The humidity data was treated in the same way as the wind speed.

#### 4.3.6. Silica concentrations

The silica concentrations in the Haldenbach micro-catchment were measured once every 3 hours. However, for some days no 3- hour data is available (Figure 4.4). The figure also shows the dynamic of the silica concentrations; when there is a peak in the discharge, a minimum of the silica concentration occurs. This effect is caused by the large amount of precipitation water in the discharge, which lowers the concentration because rain or snow has a silica concentration of about 0 mg/l. This effect should also be visible in the output of the model, including the silica module.

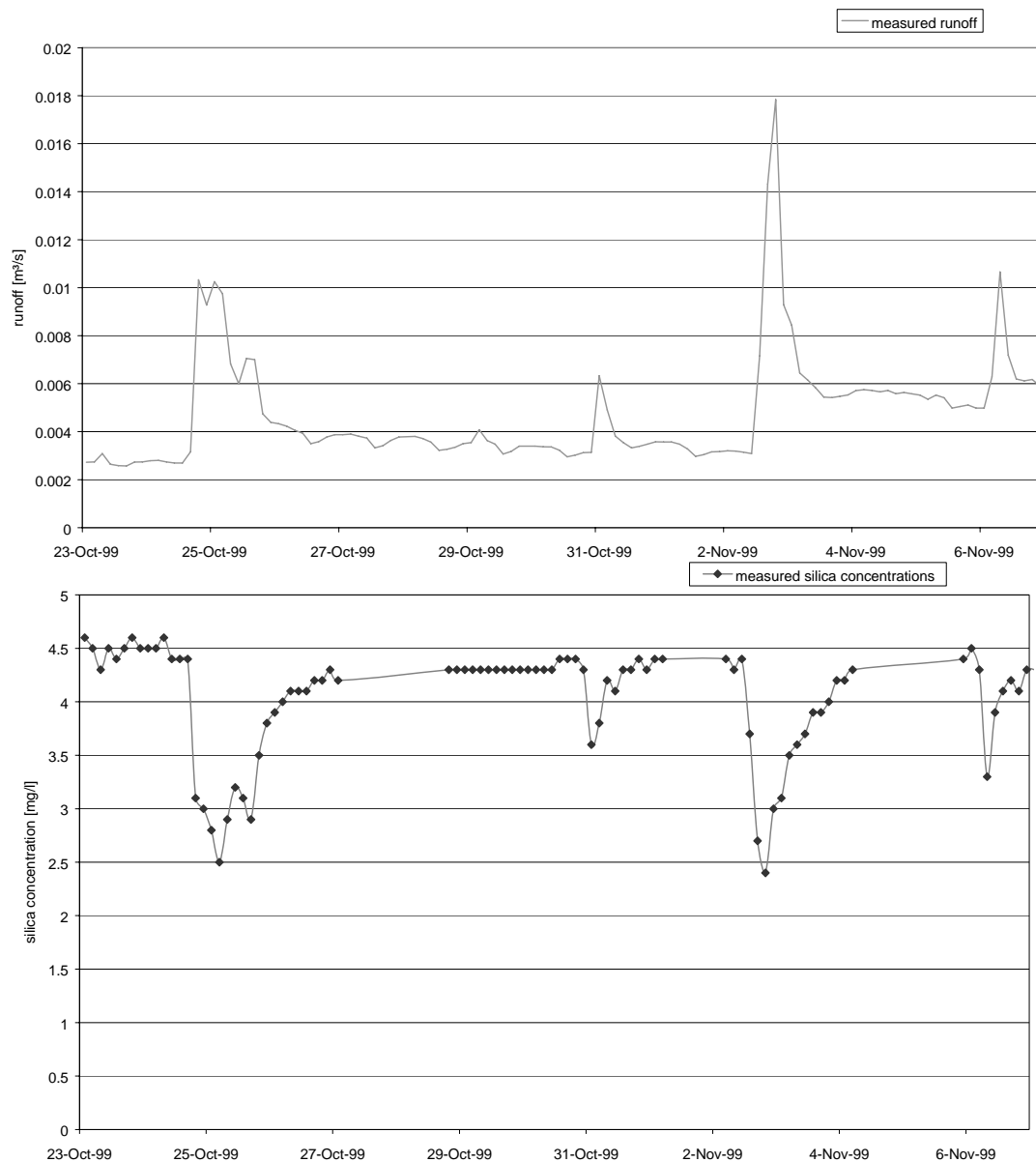


**Figure 4.4 Measured silica concentrations and discharge at gauging station OM**

#### 4.4. Initial water storage

TAC-D is a dynamic model that requires an initial storage to be defined. If this initial water storage is not adequately defined, calibration can not be done properly. Therefore an initialisation run was used to obtain a realistic filling of the boxes for the calibration run. Before the run of the initialisation period, each box was assumed to have a certain storage

(mm). For the *sGW\_box* this is 80 mm, for the *sMTD\_box* 10 mm, and 0 mm for the other boxes (*sUS\_box*, *sLS\_box* and the soil moisture storage). After this run, a map layer was produced defining the initial storage per cell for each type of storage. These so-called initial maps were used as input for the calibration period.

## 4.5. Time discretization

### 4.5.1. Modelling period

The modelling period that was used in this research was restricted by the observation period. Because only data was available for the Haldenbach micro-catchment for the period 23 October until 6 November 1999, the total modelling time is only 15 days.

### 4.5.2. Initialisation

No data from the period directly before 23 October 1999 was available for the initialisation of the model. Therefore, data from June and August 1999 was used. Unfortunately this did not lead to adequate initial values, therefore data from the observation period (23 October – 6 November 1999) was used for the initialisation.

### 4.5.3. Calibration and Validation period

The observation period consists only of 15 days (360 h), which makes it difficult to have a long calibration period, because data is also needed for validation. Therefore, 160 timesteps of 1 h were used for the calibration period, leaving 200 timesteps for the validation period. This split was made to include the large discharge peak (no. 2, Figure 4.3) and the small peak (no. 1) in the calibration period and to have sufficient data to calibrate the base flow. The problem that the small peak (no. 3) also falls into this period was not to overcome, because otherwise the period for calibrating the base flow would be too short.

The calibration was done by trial-and-error; the simulated discharge was compared with the measured discharge. Calibration objectives were the timing of the peak, the height of the peak and the recession tails.

## 4.6. Criteria for model performance

There are different criteria to investigate how a model performs. First, there is the visual check of the form of the hydrograph. The timing of the peaks, the amount of water in the peaks and the amount of water in the base flow are hereby important. The model efficiency can also be calculated; in this research, the equation of Nash and Sutcliffe (Eq. 4.1) was used (Nash & Sutcliffe, 1970).

$$R_{eff} = 1 - \frac{\sum_{i=1}^n (Q_{sim_i} - Q_{obs_i})^2}{\sum_{i=1}^n (Q_{obs_i} - \overline{Q_{obs}})^2} \quad \text{Equation 4.1}$$

With:  $R_{eff}$  = coefficient of Nash and Sutcliffe; <1 or 1 when  $Q_{sim} = Q_{obs}$   
 $Q_{sim}$  = simulated discharge [m<sup>3</sup>/s]  
 $Q_{obs}$  = measured discharge [m<sup>3</sup>/s]  
 $\overline{Q_{obs}}$  = average measured discharge [m<sup>3</sup>/s]

When the simulated hydrograph is the same as the observed hydrograph, the model efficiency is equal to 1. The lower the efficiency the less the model performs. Consequently, when  $R_{eff}$  is negative, the model efficiency is not relevant because the model output does not resemble the measured discharge.



Another measuring instrument for model performance is the volume error. The volume error is calculated by comparing the difference in the measured and the simulated discharge (Eq.4.2).

$$VE = \frac{Q_{obs} - Q_{sim}}{Q_{obs}} \cdot 100\% \quad \text{Equation 4.2}$$

With:  $VE$  = volume error [%]  
 $Q_{sim}$  = simulated discharge [mm/h]  
 $Q_{obs}$  = measured discharge [mm/h]

In this research different forms of the VE were defined, the mean VE per hour, the total VE over the calculation period, and the absolute mean VE and the absolute total VE. The latter were added because the volume error can have positive and negative values and these together could annul each other.

## 5. Extensions to TAC-D

In this chapter the adjustments to TAC-D, which were made in this research, are described. Two different modules are developed. One module to reflect the spatial variability of the riparian area and one module to simulate the silica flow in the model. The water balance was used to check on programming errors in the two modules.

### 5.1. Water balance check

TAC-D calculates different components of the water balance. The water balance as it is used in TAC-D, is described in Eq. 5.1.

$$\Delta S = P - ET_{act} - Q_{instream} \quad \text{Equation 5.1}$$

With  $\Delta S =$  storage change [mm]  
 $P =$  precipitation [mm]  
 $ET_{act} =$  actual evapotranspiration [mm]  
 $Q_{instream} =$  outflow into stream [mm]

The storage at the begin and the end of the simulation period are also stored, this amount is compared to  $\Delta S$  and the difference is the error in the water balance. Theoretically, this difference should be equal to zero; else water is created or vanished in the model.

### 5.2. Spatial variability of the riparian area (SVRA-module)

#### 5.2.1. Concept of the riparian area

Field observations in May 2002 showed that the riparian area in the Haldenbach micro-catchment can be divided into two different areas; a permanent wet area, with water standing on the surface and semi-dry organic bulbs. Therefore, it seems to be justified to change the original concept of one Micro Topographic Depression box (*sMTD\_box*) into 2 boxes. A Wet Storage box (*sMTD\_WS\_box*, or *WS\_box*), representing the saturated areas and a Dry Storage box (*sMTD\_DS\_box*, or *DS\_box*), representing the dry bulges (Figure 2.4).

#### 5.2.2. The former MTD concept

The former *sMTD\_box* (Figure 5.1), was designed in such a way that it has a limited filling height (*cMTD*) (Roser *et al*, 2001). When this filling height is exceeded, the box starts to flow over, leading this water without a time lag to the next box or to the stream (Ch. 3.2). The normal outflow is controlled by a hydraulic conductivity (*cMTD\_K*) and the stored water (*sMTD\_box*), which leads to a delay. The evaporation is assumed to be equal to the potential evaporation (*sPotET*), because of the assumption of permanent saturation of the riparian area.

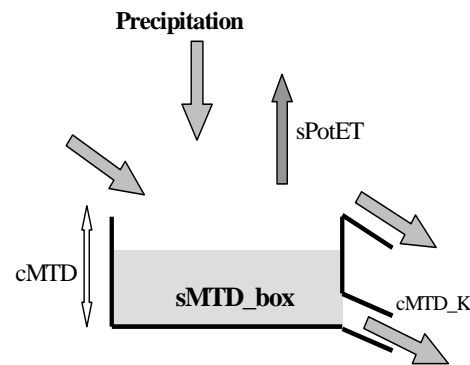


Figure 5.1 Former MTD storage concept

#### 5.2.3. The new MTD concept

The new MTD concept (Figure 5.2) consists of two different boxes which approaches the field observations better (SVRA-module). The Wet Storage box (*sMTD\_WS\_box*) looks like the former *sMTD\_box*, but now it only receives a fraction of the precipitation. With this fraction (Eq.5.2), the increase and decrease of the wet area can be simulated. Instead of changing the areas of the wet box and the dry box in the model, only the amount of water

allocated to the wet and dry box is adjusted by means of the *sMTDFraction*. The evaporation from the Wet Storage box is potential, but the potential evaporation is multiplied by the *sMTDFraction*, because only a fraction of the area can evaporate potentially.

The Dry Storage box (*sMTD\_DS\_box*) has a different setup. The evaporation from this box is not always potential, because this soil is not always saturated. The evaporation is calculated from the soil moisture content of the Dry Storage box. For that, the precipitation leading to the soil moisture storage is already corrected by the *sMTDFraction*. The evaporation from the Dry Storage box is not corrected by this fraction again. The actual evaporation of the Dry Storage box has a maximum of  $1 - sMTDFraction$  of the potential evaporation from the riparian area. This is done to prevent that the evaporation of the total area of the riparian area (sum of the evaporation from the Wet Storage box and the Dry Storage box) is higher than the potential evaporation.

Another difference between the wet box and the dry box is that the Dry Storage box has a larger storage capacity. The Dry Storage box can hardly ever flow over. The overflow option was only implemented for the unlikely event that all of the riparian area would be saturated, including the dry boxes. In that case, the dry box will also flow over.

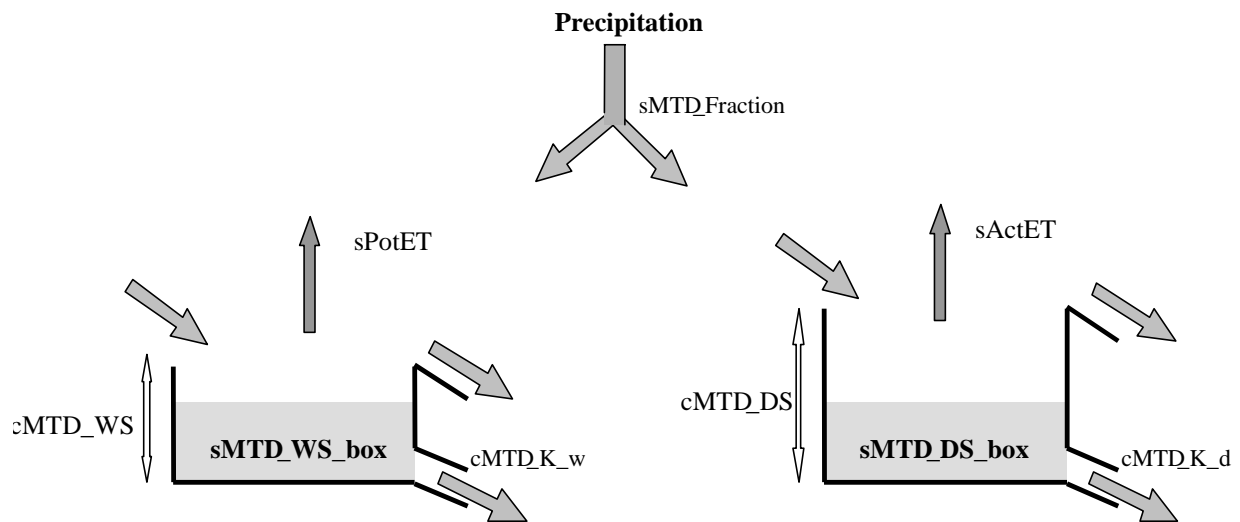


**Figure 5.2 New MTD storage concept**

The proportion of the precipitation of water to the Wet Storage box and to the Dry Storage box is calculated with the *sMTDFraction*. This fraction depends on the saturation degree of the area. The assumption is that always 30% of the area is completely saturated (lower limit) and not more than of 80% of the area can be saturated (upper limit). The fraction is calculated from the amount of water in the Wet Storage box. When the Wet Storage box is filled with 0-10 mm (initial value) the fraction is 0.3, when the box is completely full the fraction is 0.8. The intermediate values can be found with the following equation:

$$sMTDFraction = 0.3 + \frac{(sMTD\_WS\_box - 10)}{2 \cdot (cMTD\_WS - 10)} \quad \text{Equation 5.2}$$

With: *sMTDFraction* = the fraction of water the Wet Storage box receives [-]  
*sMTD\_WS\_box* = the amount of water in the Wet Storage box [mm]  
*cMTD\_WS* = the maximum filling height of the Wet Storage box [mm]

No hydraulic connection is made from the Wet Storage box to the Dry Storage box. This is left out, because in reality, when water is flowing from the wet to the dry box, the wet area increases and the dry area decreases. This increase and decrease of the area is already integrated in the model by the division of water over the *sMTDFraction*. The integration of

the SVRA-module in TAC-D is presented in Figure 5.3. The source code can be found in Annex D.

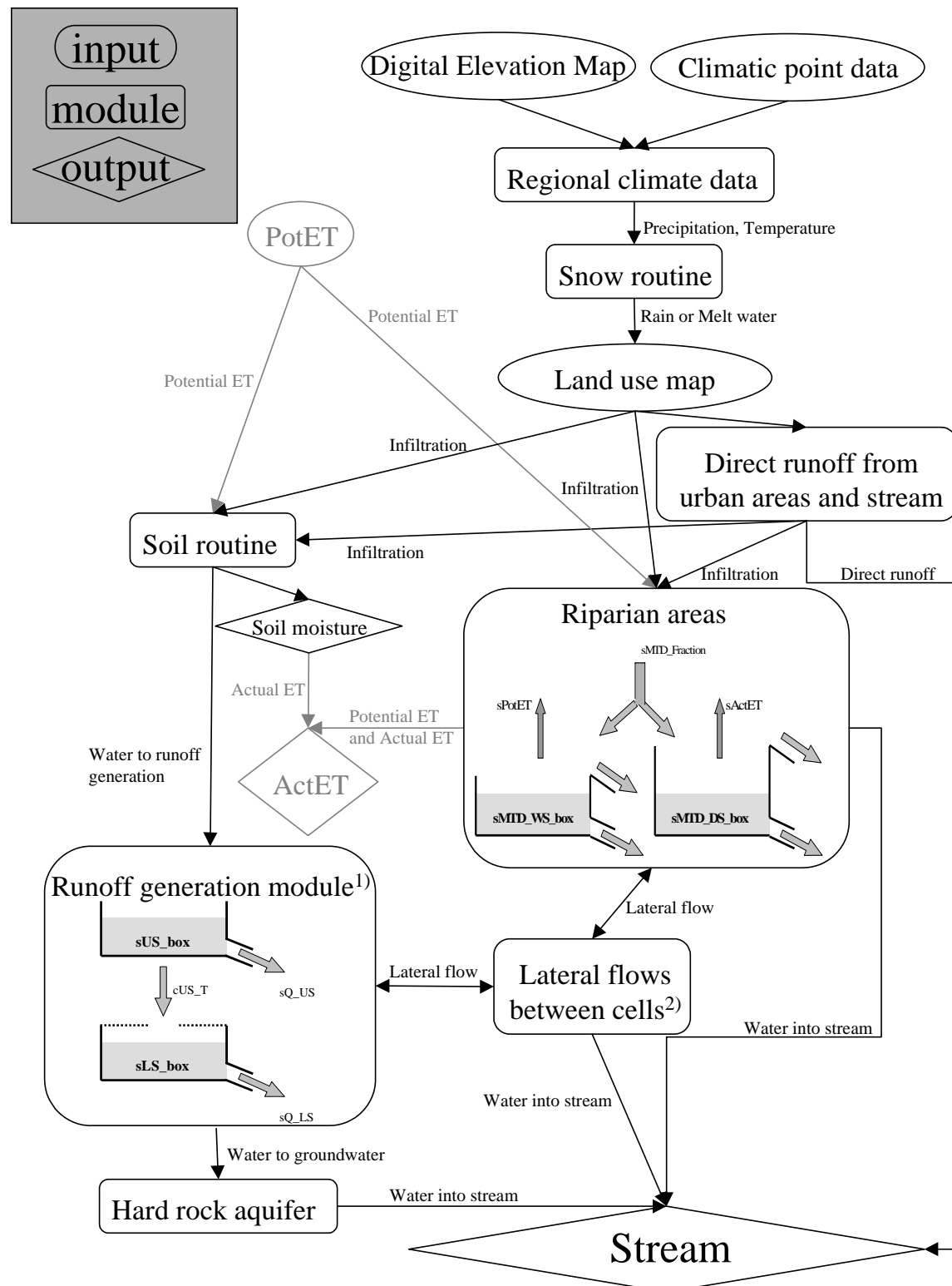


**Figure 5.3 Revised flow diagram of TAC-D; SVRA-module is included (grey box contains legend)<sup>1 2</sup>**

<sup>1</sup> Not all runoff generation zones have a lower box (Ch 3.2.7)

<sup>2</sup> This box represents the water flowing from runoff generation cells to riparian areas and vice versa

### 5.3. Integration of silica in the revised TAC-D model

#### 5.3.1. Introduction to the silica module

During the autumn of 1999, silica concentrations were measured in the Haldenbach micro-catchment (Sieder *et al.*, 2000). To simulate the silica concentrations in the stream, a module was developed. With this module, another validation possibility for the flow simulation with TAC-D is introduced. The description of silica flow can be found in Ch. 3.3.

#### 5.3.2. Concept of the silica module

The concept of the silica module was kept very simple. The concentrations of the different flow patterns (Table 3.1) were adjusted to be used in the model. For each box, a specific silica (Si) concentration was defined. Water from the groundwater box (*sGW\_box*) has the longest residence time. This water has the highest Si concentration, i.e. 6 mg/l. The runoff generation zones (except the riparian areas), are divided in Upper Storage boxes (*sUS\_box*) and Lower Storage boxes (*sLS\_box*) (Ch.3), where the lower box represents the more delayed outflow. Therefore, the *sLS\_box* is assumed to have a silica concentration almost equal to the *sGW\_box*, i.e. 5 mg/l. This value is not derived from Table 3.1, but it is an arbitrary value, assumed from the characteristics of the lower storage box. The *sUS\_box* represents a quicker flow path and has therefore a lower concentration of 3.2 mg/l. The riparian area (*sMTD\_box*) has a silica concentration of 0.3 mg/l, caused by the small residence time (Table 3.1). In the SVRA-module, both MTD boxes (*sMTD\_WS\_box* and *sMTD\_DS\_box*) are supposed to have a silica concentration of 0.3 mg/l. The precipitation has a value of 0 mg/l. The concentration per type of box does not vary; the mixing takes place when the water flows out of the box, according to equation 5.3.

$$Si_{conc} = \frac{\sum(Si_{box} \cdot Q_{out})}{Q_{tot}} \quad \text{Equation 5.3}$$

with:

- $Si_{conc}$  = the silica concentration at the gauging station [mg/l]
- $Si_{box}$  = the silica concentration of the runoff generation zone box [mg/l]
- $Q_{out}$  = the amount of water coming from that box [l]
- $Q_{tot}$  = the total amount of water at the gauging station [l]

Equation 5.3 means that the outflow is transformed into milligram Si by multiplying the concentration ( $Si_{box}$ ) with the quantity of water flowing out of the box ( $Q_{out}$ ). These milligrams are added up and then divided by the total amount of water ( $Q_{tot}$ ). The mixing of the different concentrations is performed over the local drain direction network (ldd). In Figure 5.4 the total concept is shown.

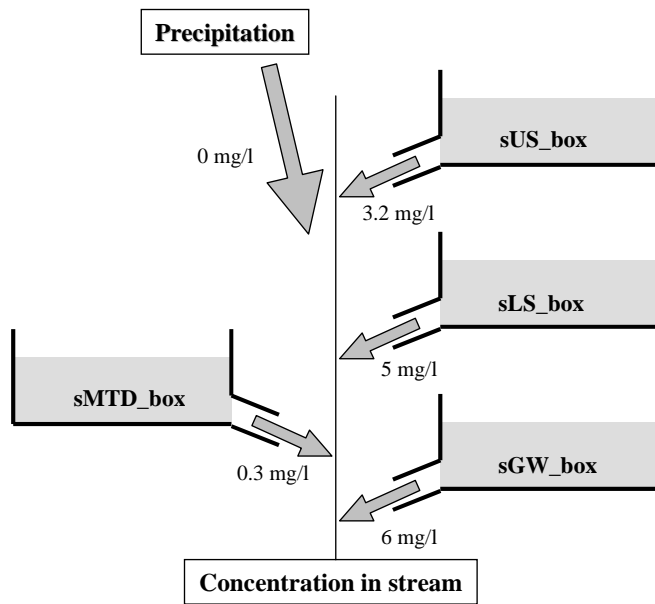


**Figure 5.4 Concept of the silica module**

A small example is given in Figure 5.5. For this example, it is assumed that there is no rain and that 1 l water is flowing out of each box. In this case, the water from Box B has a silica concentration of 3.2 mg/l. When this water flows to Box C, it will get a concentration of 0.3 mg/l, because the concept states that the concentrations in a box do not vary. The total concentration in the stream is therefore only defined by the concentrations of the water coming from Box A and Box C. These concentrations are both 0.3 mg/l, so subsequently, the water in the stream has a concentration of 0.3 mg/l.

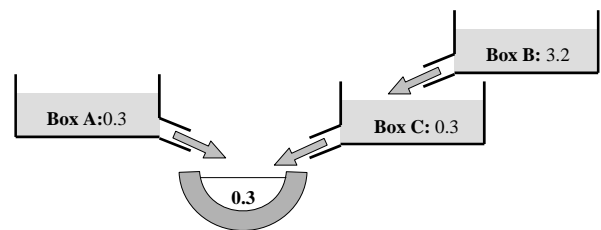


**Figure 5.5 Example of the silica module**

## 6. Results

### 6.1. Original TAC-D model

First, the model was run with the parameters identified for the Brugga catchment (Annex C). The simulated stream flow with this model version is given in Figure 6.1. The general shape of the hydrograph is reasonably well simulated, but the base flow is too low and the peaks are too high. Next, the model was calibrated (Table 6.1), hereby only the parameters for overflow of the Micro Topographic Depression box (storage capacity  $pMTD$ ) and the hydraulic resistance of the groundwater box ( $pGW\_K$ ) were adjusted. These parameter values were found by calibration. In Figure 6.2, the simulated hydrograph is presented for the calibrated TAC-D model.

**Table 6.1 Adjusted parameters for the Haldenbach micro-catchment**

Parameter name	Original value from Brugga catchment	Adjusted value for Haldenbach micro-catchment
$cMTD$	30	45
$sGW\_K$	0.001	0.018

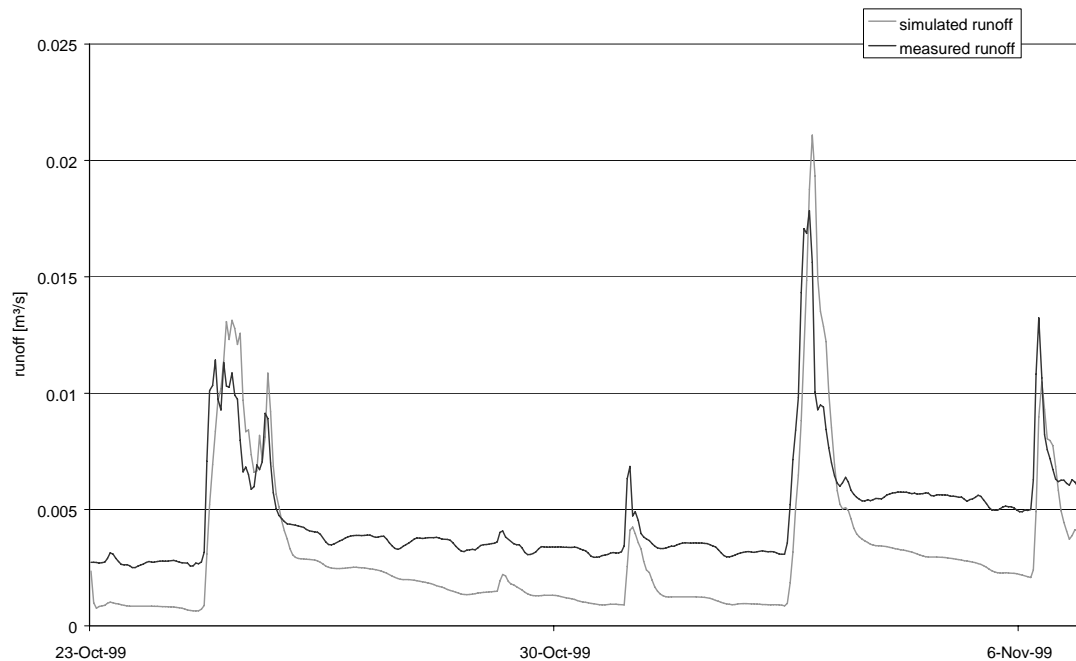


**Figure 6.1 Observed and simulated hydrographs with the original TAC-D model and original parameters**

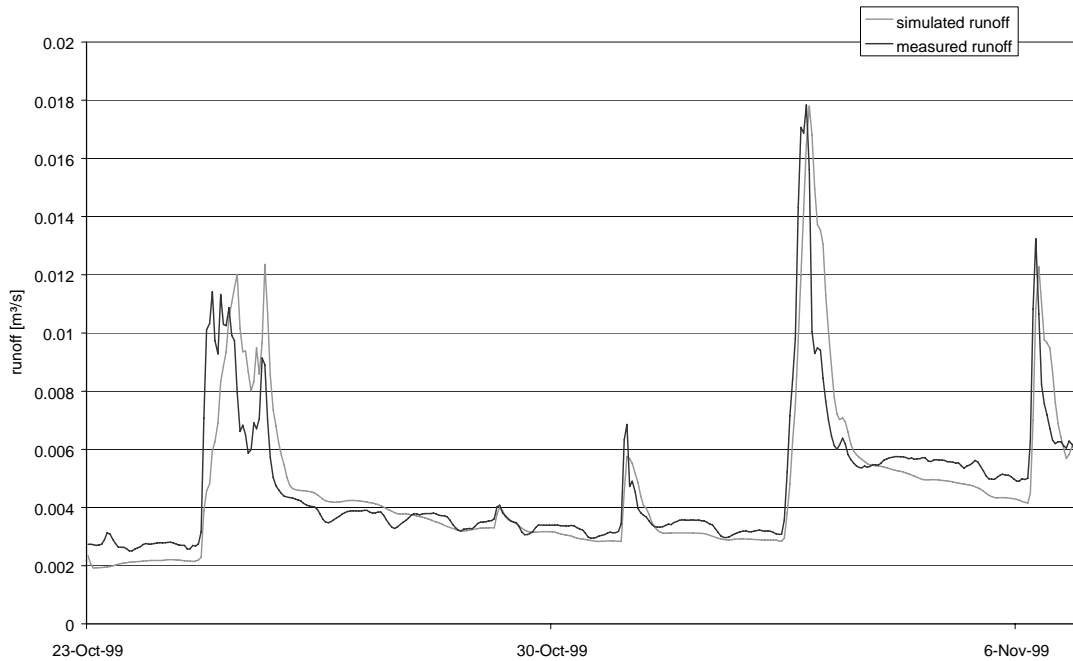


**Figure 6.2 Observed and simulated hydrographs with the original TAC-D model and adjusted parameters**

The Figures 6.1 and 6.2 show that the original TAC-D simulates the peaks on the right time. With adjusted parameters the discharge is also better simulated (Table 6.2 and Figure 6.2). The adjustment of the hydraulic conductivity of the groundwater box was done to increase the base flow. After that, the storage capacity of the *sMTD\_box* was enlarged to lower down the peaks.

**Table 6.2 Model efficiency and volume error of the original TAC-D model**

	Parameter setting					
	Original			Adjusted		
<i>Period</i>	calibration	validation	entire	calibration	validation	entire
<i>Model efficiency, <math>R_{eff}</math> [-]</i>	0.37	0.03	0.16	0.39	0.34	0.36
<i>Volume error, <math>VE</math> [%]</i>	40.4	45.4	43.5	19.0	15.3	16.8

The volume error in Table 6.2 is given in percentages. The mean volume error, the total volume error and the absolute values of the mean en total volume error can be found in Annex G.

The model efficiency and volume error of the original TAC-D model left space for improvement. Therefore the SVRA-module was developed (Ch. 5.1). The output of this module is described in the next section.

The error in the water balance for the original TAC-D and the original TAC-D with adjusted parameters is approximately 0 (Annex E).



## 6.2. Revised TAC-D model with the spatially variable riparian area module

The calibration of the revised TAC-D model with the spatially variable riparian area module (SVRA-module) was mainly based on the calibrated values the original TAC-D model (Ch. 6.2). Only a limited group of parameters was adjusted, i.e. the parameters of the riparian area (MTD boxes), the hydraulic conductivity of the periglacial drift cover ( $cP\_K\_u$ ) and the conductivity of the groundwater box ( $cGW\_K$ ) (Table 6.3). These parameters were chosen for several reasons: the MTD parameters due to the revision of the concept of the *sMTD\_box*, the hydraulic conductivity of the groundwater box ( $cGW\_K$ ) because of the effect of this parameter on the base flow, and the hydraulic conductivity of the upper storage of the periglacial drift cover ( $cP\_K\_u$ ), for the large area of this runoff generation zone in the micro-catchment.

$cMTD\_WS$  is the storage capacity of the Wet Storage box of the riparian area. This storage capacity is kept very small, because this area is assumed to be almost saturated. This means that when precipitation falls on the area, direct runoff is generated. In the concept, this small storage causes that the box starts to run over almost without a time lag, when precipitation is falling on the area.  $cMTD\_K\_w$  is responsible for the delayed outflow out of the storage. This parameter is kept very small because the less water flows out of the storage, the quicker the storage is filled during a shower and overland flow can occur.

The parameters of the Dry Storage box of the riparian area work different. This storage capacity is kept large, to approach field observations of the storage capacity of the dry bulges. The outflow of this box however is rather quick and comparable to the hydraulic conductivities of the other runoff generation zones. In general, the parameters of the Brugga were smaller due to smaller cells. The cells used in the Brugga model were 50x50 m and for the Haldenbach model only 5x5 m. This is why for instance the hydraulic conductivity of the groundwater is 10 times bigger than the value used in the Brugga model.

**Table 6.3 Adjusted parameters for the revised TAC-D model with the SVRA-module**

Parameter	Catchment (model name)	
	Brugga (TAC-D)	Haldenbach (TAC-D + SVRA-module)
$cMTD\_WS [mm]$	not present	12
$cMTD\_DS [mm]$	not present	40
$cMTD\_K\_w [h^{-1}]$	not present	0.001
$cMTD\_K\_d [h^{-1}]$	not present	0.01
$cP\_K\_u [h^{-1}]$	0.024	0.012
$cGW\_K [h^{-1}]$	0.001	0.015

After adjustment of these parameters by trial and error for the calibration period (Table 6.3), the most optimal hydrograph was found (Figure 6.3). An overview of all parameters used to run the SVRA-module can be found in Annex C.

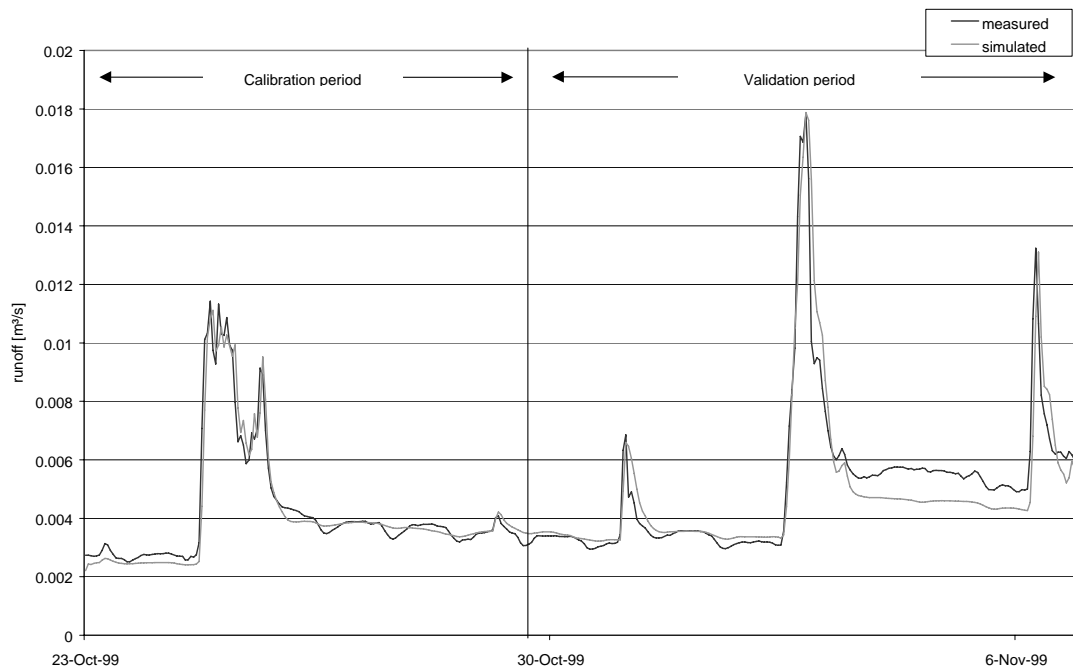


**Figure 6.3 Observed and simulated hydrographs with the revised TAC-D model including the SVRA-module**

A model efficiency ( $R_{eff}$ ) of 0.994 was reached for the calibration period. For the validation period, the results were still good with a  $R_{eff}$  of 0.927 (Table 6.4). The volume error for the calibration period was nearly 7% and for the validation period 12.5%.

**Table 6.4 Model efficiency and volume error of the revised TAC-D model with the SVRA-module**

SVRA-module parameters	Calculation period		
	Calibration	Validation	Entire
<i>Model efficiency, <math>R_{eff}</math> [-]</i>	0.944	0.927	0.933
<i>Volume error [%]</i>	6.9	12.5	10.3

The mean, total and absolute mean and total volume error can be found in Annex G. The water balance was also checked (Annex E) and the error caused by rounding off was negligible.

### 6.3. Enlarged base flow

The revised TAC-D model could not simulate the increased base flow after peak no. 5 (Figure 6.3). To see if of the measured amount of discharge was correct, the amount of water coming from the rain was compared with the amount of water in the peak. The base flow during and after peak no. 5 was assumed to be the same as before the shower (0.003 m³/s average in that hour). The discharge peak should consist of water from the shower and water from the base flow. This assumption makes it possible to define the direct discharge from the precipitation (Eq. 6.1).

$$q^*(t) = q(t) - q_b$$

**Equation 6.1**

With:  $q^*(t)$  = direct discharge from precipitation [m³/s/h]  
 $q(t)$  = measured discharge [m³/s/h]  
 $q_b$  = base flow (0.003 m³/s/h)

Two arbitrary chosen points ( $t_1$  and  $t_2$ ) define the begin and end of the peak. With use of Equation 6.2 it was then possible to calculate the amount of water coming from the precipitation by integration (Eq. 6.2) of the shaded area in the hydrograph (Figure 6.4).

$$Q_{rain}^* = \int_{t_1}^{t_2} q^*(t) \cdot dt \quad \text{Equation 6.2}$$

With:  $Q_{rain}^*$  = amount of rain estimated from hydrograph [ $\text{m}^3/\text{s}$ ]  
 $q^*(t)$  = direct discharge from precipitation [ $\text{m}^3/\text{s/h}$ ]  
 $t$  = time [h]

TAC-D converted the measured amounts of water from the hydrograph to  $\text{m}^3/\text{s}$ .  $Q_{rain}^*$  for the calculation period (29 h) was  $0.158 \text{ m}^3/\text{s} = (0.158 * 3600 * 1000 * 29) / 190400 = 87 \text{ mm}$ . The precipitation in that 29 h was 56 mm, or converted to  $\text{m}^3/\text{s}$ :  $0.102 \text{ m}^3/\text{s}$ .

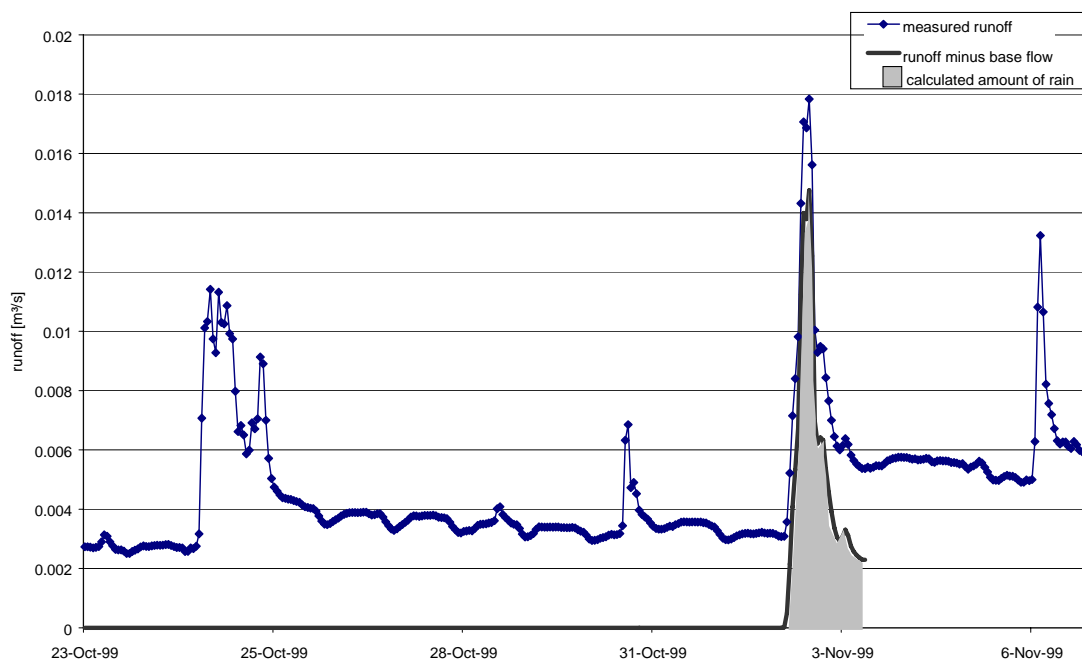


**Figure 6.4 Calculated amount of rain from the runoff**

So, there is a difference in water, the enlarged base flow cannot be caused by the rain, because the peak itself contains already more water than that is fallen as precipitation. Two explanations can be given for this difference, i.e. either the runoff or the precipitation is not measured correctly. The precipitation, however, is checked by using another climate measuring station, so the first explanation seems the most likely. It could be that there was an offset of the zero point in the base measurement.

## 7. Parameter sensitivity analysis

### 7.1. Procedure

The parameter sensitivity analysis was carried out for all the parameters adjusted for the revised TAC-D model with the SVRA-module (Table 6.3). The parameters derived from the Brugga catchment (Annex C), which were not adjusted, were not taken into account. The sensitivity analysis was carried out by running the model with higher and lower parameter values, as the ones identified for the reference model (Ch. 6.4). The percentage change was dependent on the type of parameter. The parameter adjustments were only carried out for individual parameters, so no multi-parameter sensitivity analysis was done.

### 7.2. Results

The results of the parameter sensitivity analysis are represented in Table 7.1 (on the next page) and are discussed below.

- The filling height of the Wet Storage box (*cMTD\_WS\_box*) turns out to be very sensitive. This is caused by the large effect of the storage capacity on the amount of water that is routed from the wet storage box of the riparian area into the stream. The SVRA-module is developed in such a way, that the outflow of the wet storage box of the riparian area (*cMTD\_K\_w*) is very small. Therefore, the box quickly flows over, when precipitation is falling on the riparian area. When the storage capacity is enlarged (by enlarging the *cMTD\_WS*) this overflow takes place on a later time, and model performance is worse. When a smaller parameter value was chosen than in the reference model, the concept was not working anymore (Ch. 5.1). Then Eq. 5.2, the equation that calculates *sMTDFraction*, is incorrect because *cMTD\_WS* is then smaller than the minimal value. The different hydrographs of the sensitivity analysis of this parameter are displayed in Figure 7.1.
- The filling height of the Dry Storage box (*cMTD\_DS*) is less sensitive than *cMTD\_WS*, for this box is designed in such a way that it hardly ever runs over. When this value is unrealistic high the model performance is slightly better, but the more realistic value was chosen.
- The hydraulic conductivity of the Wet Storage box (*MTD\_K\_w*) cannot be too high, because then the overflow concept does not work correctly. The model efficiency and volume error are slightly better with lower parameter values. However, the reference model was not changed after this conclusion because the lower parameter values are unrealistic and do not give a significant improvement.
- Parameter *pMTD\_K\_d* represents the hydraulic conductivity of the dry storage box of the riparian area. Both enlargement and reduction of this parameter lead to a less good fit.
- The hydraulic conductivity of the upper storage box of the periglacial cover layer (*pP\_K\_u*) was the only parameter of the runoff generation zones of the Brugga catchment that was adjusted. This parameter reacts in the same way as *pMTD\_K\_d*.
- The hydraulic conductivity of the groundwater box (*cGW\_K*) is mainly responsible for the generation of base flow. Therefore, its value has a significant impact on the simulated base flow. When this parameter is larger, the base flow is larger, when this parameter is reduced, the simulated base flow drops below the measured base flow (Figure 7.2).

**Table 7.1 Results of the parameter sensitivity analysis of the SVRA-module**

Parameter	Parameter value	Difference to the reference model [mm/h]	total VE [%]	R <sub>eff</sub> [-]
Filling height of the Wet Storage box of the riparian area [mm]				
<i>cMTD_WS</i>	24 (+100%)	0,07	12.9	0,56
<i>cMTD_WS</i>	18 (+50%)	0,03	11.4	0,79
<i>cMTD_WS</i>	12 (ref)	0,00	10.3	0,93
<i>cMTD_WS</i>	9 (-25%)	-0,27	21.6	0,13
<i>cMTD_WS</i>	6 (-50%)	-0,24	20.1	0,24
Filling height of the Dry Storage box of the riparian area [mm]				
<i>cMTD_DS</i>	80 (+100%)	-0,02	9.8	0,94
<i>cMTD_DS</i>	40 (ref)	0,00	10.3	0,93
<i>cMTD_DS</i>	20 (-50%)	0,02	11.4	0,91
Hydraulic conductivity of the Wet Storage box of the riparian area [h <sup>-1</sup> ]				
<i>cMTD_K_w</i>	0,01 (10x)	-0,01	10.8	0,84
<i>cMTD_K_w</i>	0,005 (5x)	0,00	10.5	0,90
<i>cMTD_K_w</i>	0,001 (ref)	0,00	10.3	0,93
<i>cMTD_K_w</i>	0,0005 (0.5x)	0,00	10.2	0,94
<i>cMTD_K_w</i>	0,00001 (0.1x)	0,00	10.3	0,94
Hydraulic conductivity of the Dry Storage box of the riparian area [h <sup>-1</sup> ]				
<i>cMTD_K_d</i>	0,1 (10x)	1,02	60.2	-2,39
<i>cMTD_K_d</i>	0,01 (ref)	0,00	10.3	0,93
<i>cMTD_K_d</i>	0,001 (0.1x)	-0,06	13.6	0,89
Hydraulic conductivity of the upper storage box of the periglacial cover layer [h <sup>-1</sup> ]				
<i>cP_K_u</i>	0,12 (10x)	0,95	55.8	-1,41
<i>cP_K_u</i>	0,06 (5x)	0,56	33.0	0,28
<i>cP_K_u</i>	0,012 (ref)	0,00	10.3	0,93
<i>cP_K_u</i>	0,006 (0.5x)	-0,11	13.1	0,92
<i>cP_K_u</i>	0,0012 (0.1x)	-0,21	17.2	0,88
Hydraulic conductivity of the groundwater storage [h <sup>-1</sup> ]				
<i>cGW_K</i>	0,03 (100 %)	0,79	44.4	-0,20
<i>cGW_K</i>	0,015 (ref)	0,00	10.3	0,93
<i>cGW_K</i>	0,0075 (-50%)	-0,47	31.3	0,57

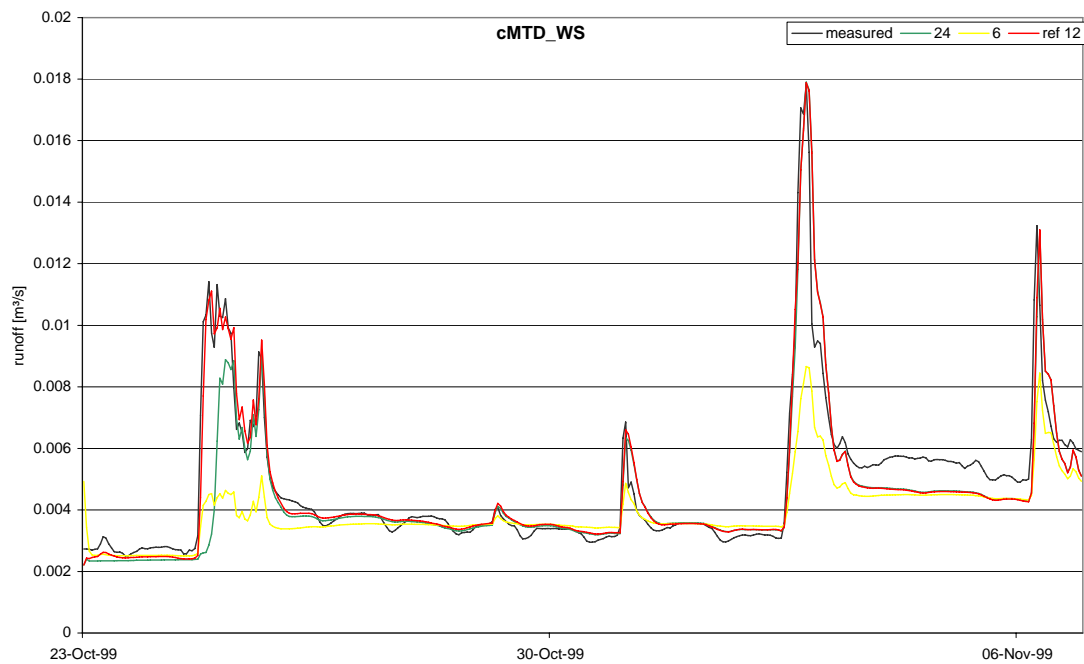


**Figure 7.1 Sensitivity of the storage capacity of the Wet Storage box of the riparian area on the simulated runoff**

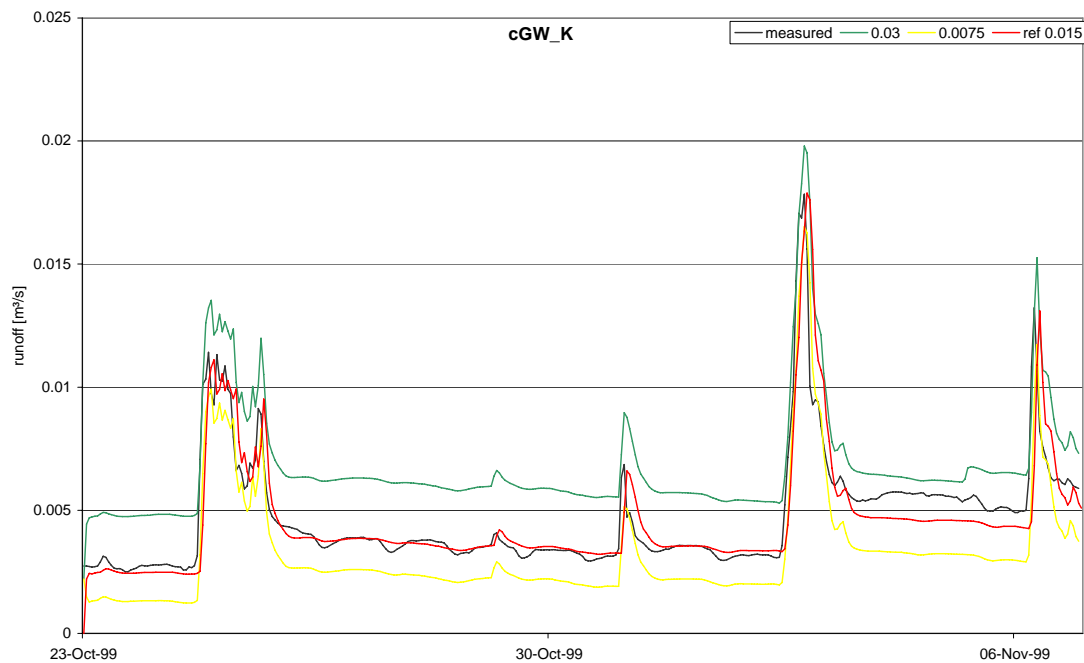


**Figure 7.2 Sensitivity of the hydraulic conductivity of the deep groundwater on the simulated runoff**

The graphs of the other parameters with the different values used in the parameter sensitivity can be found in Annex F.

## 8. Model upscaling

### 8.1. Introduction

Upscaling is performed to reduce computer calculation time, which is especially useful when the modelling period or the catchment is large. Data collection can be easier when the spatial resolution is larger. Sometimes a larger spatial resolution is even necessary because not always such detailed spatial data is available.

### 8.2. Spatial resolution from 5x5 m to 50x50 m

The original TAC-D model was developed for the Brugga catchment, which has an area of 40 km<sup>2</sup> (Roser *et al.*, 2001). This catchment was modelled in PCRaster with a raster of 50x50 m. For the Haldenbach micro-catchment this was assumed to be a too large resolution. However to see if the benefits of upscaling have not a too large effect on the model output, the revised TAC-D with the SVRA-module was also run with cells of 50x50 m.

By the conversion of the cell length, PCRaster created also cells with only a small percentage of the original area in it (Figure 8.1). Because this is not realistic, cells with more than 75 % area that not occurred on the original map were removed. This results in the map presented in Figure 8.2. Because of the larger cells, runoff generation zone no. 3 (not layered drift cover) disappeared (see also Figure 4.1).



Figure 8.1 The original catchment (5m cell length) and the new one (50 m cell length)

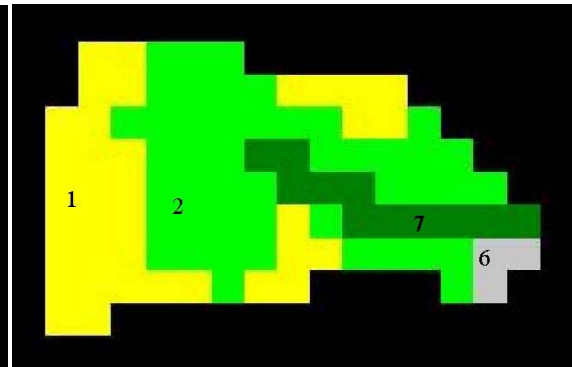


Figure 8.2 The new runoff generation zone map

Obviously, the change in cell size also affects the number of cells and the total area in the model (Table 8.1). This table displays the area derived from the topographical map (topographical map area) and the newly defined area caused by converting the area into square cells. The error percentage is also mentioned in Table 8.1. This percentage accounts for the difference between the total area calculated by PCRaster and the measured area. This is hard to overcome because the area is converted into square cells. Especially for the larger spatial resolution, the error is large.

**Table 8.1 Characteristics of the original area (cell size 5x5 m) and the upscaled area (cell size 50x50 m)**

cell length [m]	Catchment					
	MU			OM		
	Topo-graphical map area [m <sup>2</sup> ]	no. of cells [-]	total area of all cells [m <sup>2</sup> ]	Topo-graphical map area [m <sup>2</sup> ]	no. of cells [-]	total area of all cells [m <sup>2</sup> ]
5	208.000	8709	217.725 (+5%)	181.000	7616	190.400 (+5%)
50		96	240.000 (+15%)		86	215.000 (+19%)

The calculation time for the revised TAC-D model, including the SVRA-module, is 9 minutes for the catchment with a cell length 5 m, whereas it decreases to 15 seconds for a cell length of 50 m

### 8.3. Results

As described in the previous paragraph, the calculation time is reduced considerably. However, model performance was really worse compared to the model with the 5x5 m resolution.

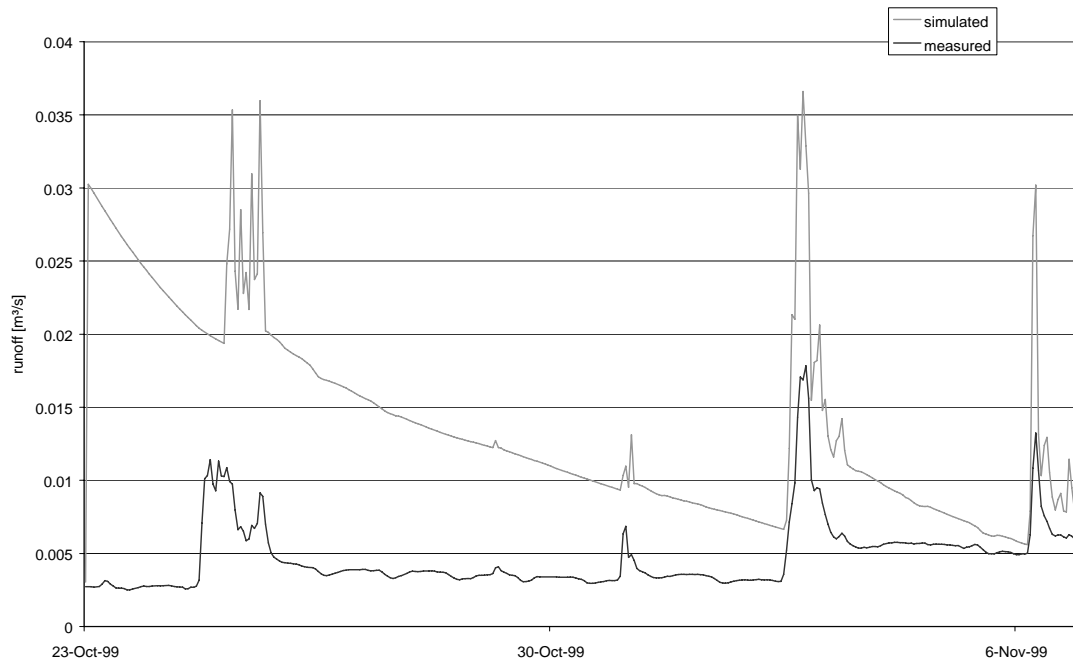


**Figure 8.3 Observed and simulated hydrographs with the revised TAC-D model including the SVRA-module with parameters of the reference model and a cell length of 50 m**

As can be seen in Figure 8.3, calibration is necessary when the cell size is changed, because the hydraulic conductivity should be smaller when the cells are enlarged. The adjusted hydraulic conductivities are presented in Table 8.2. These values were used as initial values, however, no better parameter values were found in the calibration and therefore these values were not further adjusted.

**Table 8.2 Parameters of the 5 m cell length and the 50 m cell length model**

Adjusted parameters	5 m cell length	50 m cell length (0.1x)
<i>cMTD_K_w</i>	0.001	0.0001
<i>cMTD_K_d</i>	0.01	0.001
<i>cP_K_u</i>	0.012	0.0012
<i>cGW_K</i>	0.015	0.0015

The base flow in the run with the adjusted parameters is simulated rather well (Figure 8.4), the peaks, however, are too high and the timing is less as in the model run with a spatial resolution of 5 m.



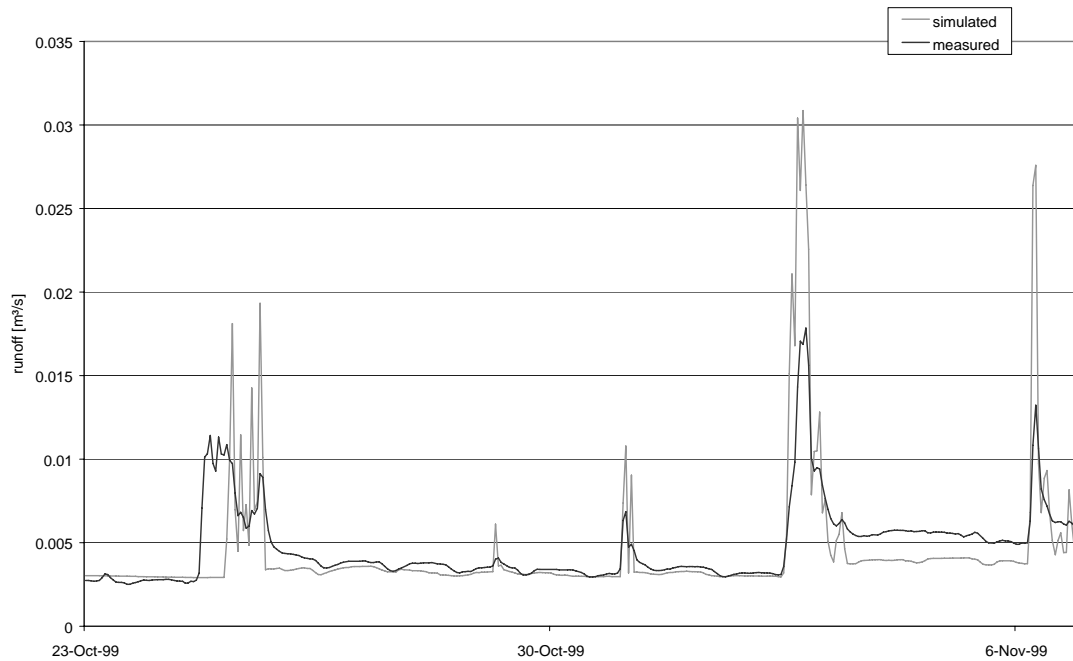


**Figure 8.4 Observed and simulated hydrographs with the revised TAC-D model including the SVRA-module with parameters ten times smaller than the reference model and a cell length of 50 m**

The model efficiency and volume error are presented in Table 8.3. The modelling efficiency has no meaning because of the large differences in the peaks of the measured and simulated runoff. The total volume error is more than 4 times larger than the volume error for the run with the smaller spatial resolution.

**Table 8.3 Performance of the model with a cell length of 5 and 50 m**

SVRA-module parameters	cell length [m]	
Cell length [m]	5	50
Model efficiency, $R_{eff}$ [-]	0.933	-0.2091
Volume error, mean VE [mm/h]	0.0009	0.0050
Volume error, total VE [mm]	0.321	1.811
Absolute mean VE [mm/h]	0.0011	0.0051
Absolute total VE [mm]	0.412	1.853

The conclusion can be drawn that upscaling for such a small catchment is no realistic option, because micro-scale processes (e.g. the flow processes in the small riparian area) are not represented correctly.

## 9. Results of the silica module

### 9.1. *Simulated silica concentrations*

The time series of the simulated silica concentrations using the silica parameters from Figure 5.4 is displayed in Figure 9.1. This figure shows that the silica concentration reacts on the amount of precipitation in the discharge, but the effect is too large. The simulated silica concentration drops to about 0.3 mg/l whereas in reality it is higher than about 2.5 mg/l (Figure 4.4). Moreover, in stead of rising to the base level, the silica concentration after a discharge peak stays low and only recovers very slowly.

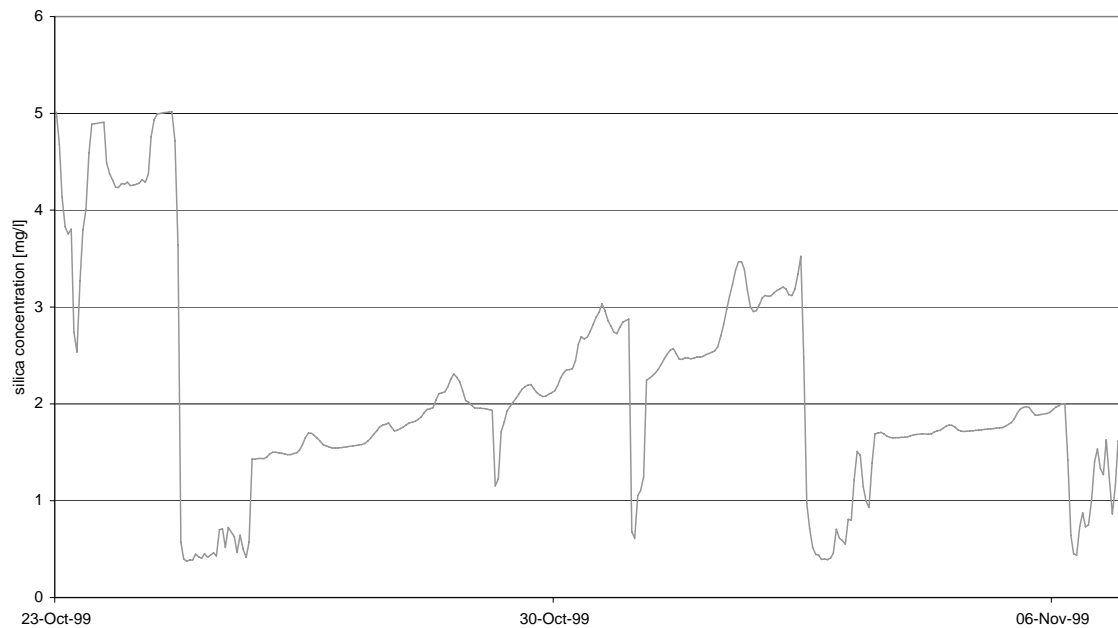


**Figure 9.1** Simulated silica concentrations at gauging station OM

### 9.2. *Sensitivity of the silica module*

To see, if this slow recovery was an effect of a wrongly chosen silica concentration from one of the boxes, all silica concentrations of the boxes individually were enlarged by a concentration of 1 mg/l and finally the silica concentration of all boxes was enlarged by 1 mg/l (Figure 9.3). This sensitivity analysis was restricted to the calibration period caused by capacity problems of the computer.

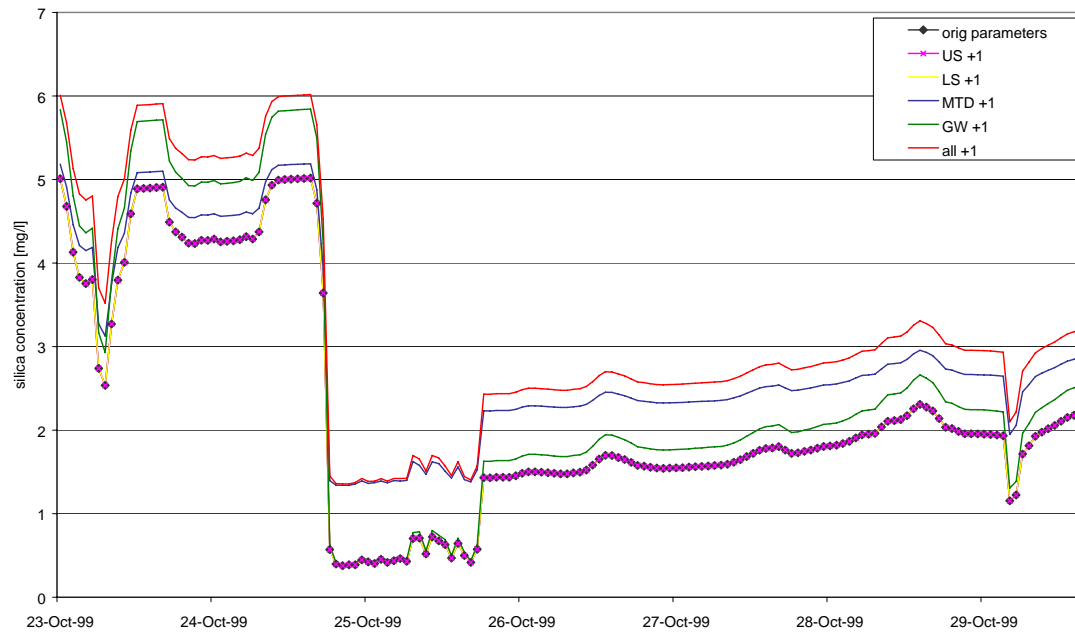


**Figure 9.2 Influence of the silica concentrations of the different boxes on the simulated silica concentrations at gauging station OM**

Figure 9.2 shows that the silica concentrations of the *sLS\_box* and the *sUS\_box* have no effect on the simulated silica concentrations. The silica concentration of the riparian area (*sMTD\_box*), however, causes a quicker recovery of the concentration of the base flow, when this parameter is enlarged to 1.3 mg/l. The silica concentration of the groundwater (*sGW\_box*) causes only an increase of the concentration during the recession. During peak discharge the effect is minimal. An increase of the silica concentration of all boxes with 1 mg/l does not give the recovery of the base flow concentration as shown in Figure 4.4.

A possible explanation could be that only the deep groundwater system (*sGW\_box*) and the riparian areas (*sMTD\_box*) are directly connected to the stream (Figure 3.9 and Figure 4.1). Consequently, only the silica concentration of the *sGW\_box* and *sMTD\_box* are responsible for the calculated concentration. The concept of the silica module (Ch. 5.2.2) states that the concentrations of the boxes are constant. So when, for instance, water from a periglacial drift cover cell (4.2 mg/l) flows into an adjacent downstream cell of the riparian area, the concentration of this water is neglected and the water gets the concentration of the *sMTD\_box* [0.3 mg/l]. Therefore, it is clear that the silica module is not working correctly. In further research a new concept need to be developed, which does include the mixing of the concentrations within the boxes.

## 10. Conclusions and recommendations

### ***Original TAC-D***

The first impression is that the original TAC-D, after calibration of the parameters, simulates the discharge rather well (Figure 6.2). However, the model efficiency is not so good ( $R_{\text{eff}} = 0.35$ ) and the volume error is rather large (6 mm).

### ***SVRA-module***

The newly developed SVRA-module works very good for the modelling period of 15 days for the Haldenbach micro-catchment. A with a model efficiency of 0.93 and a volume error of 0.4 mm is reached. However, the parameters are very dependent of the chosen spatial resolution and when this module is applied to another catchment with a different cell size, new calibration is necessary.

The period of 15 days used in this research is rather short to draw firm conclusions on the general use of the SVRA-module. Further research with longer time series is necessary to draw that conclusion.

Unfortunately gauging station MU only functioned for a very short period. When it had been operating for a longer time, it had been possible to enclose a small catchment (MU-OM) with a large area of riparian zones, to get an even better view on the reliability of the SVRA-module. In further research, it is recommended that field data of such a catchment are collected to test the SVRA-module.

### ***Sensitivity of the parameters of the SVRA-module***

The model performance is worse when the hydraulic conductivity from a box is enlarged or decreased. There is only one exception, namely, the conductivity of the Wet Storage of the Micro Topographic Depression box. When the conductivity of this box is decreased, model performance slightly improves. This is caused by the developed concept. When the hydraulic conductivity is smaller, more water is transported through the overflow (overland flow), and leaves the box without a time lag.

### ***Upscaling from a 5 m cell length to a 50 m cell length***

The upscaling in this research was performed to see the effect on model performance of the TAC-D model, including the SVRA-module when the area has a larger spatial resolution. The amount of cells hereby decreased from almost 9000 to 90 cells. Because of the 100 times larger resolution, the hydraulic conductivities had to be adjusted. After adjustment and calibration, the model performance was still not very well. The simulated base flow was simulated rather well, but the peaks were too high and the timing of the peaks was less than in the model run with the smaller spatial resolution. Therefore, upscaling for such a small catchment leads to lower model performance because micro-scale processes (e.g. in the riparian areas) are not represented correctly.

### ***Silica module***

This module was developed to have an extra validation possibility for the simulation of the contribution of each runoff generation zone to the stream flow. Each box was assigned a silica concentration and these concentrations were assumed to be constant within the box. The results of this module were not as expected. The silica concentrations became too low during a peak discharge and recovered too slowly to the base level. The assumption is that this effect is caused by the constant concentrations within the boxes. Further research should confirm this.

### ***Final conclusion***

The revised TAC-D model, including the SVRA-module, gives good results for the application to the Haldenbach micro-catchment for the period 23 October – 6 November. This

however, is a very short period and therefore the developed module should also be tested on a catchment where data is available for a longer period. Furthermore, the parameters are very scale dependent and have no real physical meaning. An effect of the scale dependency of the parameters is that calibration is necessary when the model is applied to another catchment. Therefore the use of this model is limited to a better understanding of the hydrological processes in a catchment but it makes it difficult to use the model for predicting the reaction of the catchment to changes.

## References

---

- Allen, R.G., Pereira, L.S., Raes, D., Smith, M.** (1998) Crop evapotranspiration - Guidelines for computing crop water requirements - *FAO Irrigation and drainage paper 56*, p17-28  
*Rome*
- Appelo, C.A.J. & Postma, D.** (1999) Geochemistry, groundwater and pollution. A.A. Balkema, Rotterdam, p202-237.
- Dam, O. van** (2000) Modelling incoming Potential Radiation on a land surface with PCRaster. *Environmental GeoSciences, Faculty of Earth- & Life Sciences Vrije Universiteit Amsterdam* <http://www.geo.vu.nl/~damo/potrad/potrad.htm> [access date: 6-5-2002]
- Deursen, W.P.A. van** (1995a) Water balance studies of large river basins with respect to their sensitivity to climate changes- section 6.2: Implementation of the RHINEFLOW. *PhD thesis Faculty of Physical Geography, University of Utrecht*. Internet: <http://rhine.geog.uu.nl/modelscrip.html> [access date: 2-4-2002]
- Deursen, W.P.A. van** (1995b) Geographical Information Systems and Dynamic Models. Development and application of a prototype modelling language. *PhD thesis, Faculty of Spatial Sciences University of Utrecht*. Internet: . <http://www.geog.uu.nl/pcraster/thesisWvanDeursen.pdf> [access date: 2-4-2002]
- Hoeg, S., Uhlenbrook, S., Leibundgut, Ch.** (2000) Hydrograph separation in a mountainous catchment – combining hydrochemical and isotopic tracers. *Hydrological Processes 14*, p1199-1216.
- Nash J.E. & Sutcliffe J.V.** (1970) River flow forecasting through conceptual models; 1, a discussion of principles. *J. Hydrol. 10* (3), 282-290.
- PCRaster Research Team** (unknown year) PCRaster Version 2 Manual. *Faculty of Geographical Sciences, University of Utrecht*. Internet: <http://pcraster.geog.uu.nl/manuals/pcrman/book1.htm> [access date 2-4-2002]
- Ott, B., Uhlenbrook, S., Leibundgut Ch.** (2002) Weiterentwicklung des Einzugsgebietsmodells TAC-D und Anwendung im Dreisameinzugsgebiet *Diplomarbeit Insitut für Hydrologie, der Albert-Ludwigs-Universität Freiburg i. Br.*
- Roser, S., Uhlenbrook, S., Leibundgut, Ch.** (2001) Flächendetaillierte Weiterentwicklung des prozessorientierten Einzugsgebietsmodells TAC und Visualisierung der Modellergebnisse in einem dynamischen GIS. *Diplomarbeit Insitut für Hydrologie, der Albert-Ludwigs-Universität Freiburg i. Br.*
- Sieder, M., Demuth, S., Leibundgut, Ch.** (2000) Experimentelle Untersuchung der abflussbildung auf Sättigungsflächen. *Diplomarbeit Insitut für Hydrologie, der Albert-Ludwigs-Universität Freiburg i. Br.*
- Uhlenbrook, S. & Leibundgut, Ch.** (1997) Abflussbildung bei Hochwasser in verschiedenen Raumskalen. *Wasser & Boden, 49 jahrg.*, p 13-22, 9/1997.
- Uhlenbrook, S.** (1999) Untersuchung und Modellierung der Abflussbildung in einem mesoskaligen Einzugsgebiet. *Freiburgers Schriften zur hydrologie, band 10, Albert-Ludwigs-Universität Freiburg i. Br.*

**Torfs, P.J.J.F.** (2001) Stroming in open water. *Lecture notes of department of water resources, Wageningen University.*

## Annexes

---

<b>Annex A</b>	Morphologic characteristics of the total and the two different sub-catchments of the Haldenbach micro-catchment
<b>Annex B</b>	Precipitation in the Haldenbach micro-catchment from 21 October to 9 November 1999
<b>Annex C</b>	Parameters defined for the Brugga catchment
<b>Annex D</b>	Syntax SVRA-module
<b>Annex E</b>	Water balances for the different modules
<b>Annex F</b>	Hydrographs of the parameter sensitivity analysis
<b>Annex G</b>	Model performance parameters



**Annex A Morphologic characteristics of the total and the two different subcatchments of the Haldenbach micro-catchment**

Catchment characteristics	Catchment		
	MU	OM	MU-OM
area [m <sup>2</sup> ]	208000	181000	27000
max. elevation a.m.s.l. [m]	1168	1168	1126
min. elevation a.m.s.l. [m]	1079	1090	1079
difference between max. and min. elevation [m]	89	78	47
mean slope [%]	9,5	7,5	16
max. length slope [m]	752	64	312
length of the stream [m]	420	305	115

# Annex B Precipitation in the Haldenbach micro-catchment from 21 October to 9 November 1999

event characteristics	Event number					
	1	2	3	4	5	6
period	23-10-1999 05:40-07:40	24-10-1999 15:40 - 25-10-99 16:50	29-10-99 03:20-06:20	31-10-99 01:10 - 04:50	2-11-1999 11:50 - 3-11-99 10:30	6-11-99 4:30-19:50
duration [h]	2h	25h, 10min	3h	3h, 40min	22h, 40min	15h, 20min
sum [mm]	1,2	63,9	1,7	10,2	57,3	20,3
mean intensity [mm/h]	0,6	2,54	0,56	2,78	2,53	1,32

**Annex C Parameters defined in the original TAC-D model for the Brugga catchment  
(Roser, 2001)**

<b>Parameter</b>	<b>Name</b>	<b>Unit</b>	<b>Value</b>
<b>Microtopographic depression box</b>			
Storage boundary	cMTD	[mm]	45
Hydraulic conductivity	cMTD_K	[1/h]	0,01
<b>Flat hilltops</b>			
Hydraulic conductivity	cH_K	[1/h]	0,001
<b>Periglacial drift cover</b>			
Hydraulic conductivity of upper storage	cP_K_u	[1/h]	0,024
Hydraulic conductivity of lower storage	cP_K_l	[1/h]	0,005
Storage boundary of lower storage	cP_H	[mm]	400
Percolation from upper to lower box	cP_T	[1/h]	0,2
<b>Not-layered drift cover</b>			
Hydraulic conductivity of upper storage	cD_K_u	[1/h]	0,2
Hydraulic conductivity of lower storage	cD_K_l	[1/h]	0,024
Storage boundary of lower storage	cD_H	[mm]	80
Percolation from upper to lower box	cD_T	[1/h]	0,6
<b>Boulder field</b>			
Hydraulic conductivity	cB_K	[1/h]	0,2
<b>Accumulation zone at foothills</b>			
Hydraulic conductivity of upper storage	cF_K_u	[1/h]	0,2
Hydraulic conductivity of lower storage	cF_K_l	[1/h]	0,007
Storage boundary of lower storage	cF_H	[mm]	150
Percolation from upper to lower box	cF_T	[1/h]	0,6
<b>Moraine area</b>			
Hydraulic conductivity	cM_K	[1/h]	0,002
<b>Hard rock aquifer</b>			
Hydraulic conductivity	cGW_K	[1/h]	0,018
Storage boundary	cGW_H	[mm]	1000
Percolation to groundwater (not for MTD)	cAll_P	[1/h]	0,075
<b><i>For all upper storage boxes</i></b>			
Storage boundary upper storage	cUS_H	[mm]	800

## Annex D Syntax of the SVRA-module

```
*****
# MTDFraction of the SOF_zone
*****
sMTDFraction =if (sMTD_WS_box le 10, 0.3,(0.3+((sMTD_WS_box-10)/(2*(cMTD_WS-
10)))));
sMTDFraction =min(0.8, areaaverage (sMTDFraction,bSOF_zone)); #maximal 80% of the
SOF area will be completely saturated

*****
# Soil routine (for all zones except zones of wet saturated overland flow)
*****
# Save present soil moisture at begin of timestep
sSoilMoistureAtBegin = sSoilMoisture;

# Calculate changing soil moisture content (after adding one mm infiltrated water a time)and
percolating water to runoff generation routine using two external functions
sInSoilold = sInSoil;
sInSoil = if (defined (bSOF_zone), (sInSoil*(1-sMTDFraction)), sInSoil); #the SOFzone
becomes only a fraction of water for the soil routine (only the water to the dry box goes
through the soilroutine)

*****
# Zone of saturated overland flow (SOF)
*****

*****
# SOF, Wet zone Storage (WS)
*****
# Input of rain or meltwater into "micro-topographic depression" storage (mm)
sMTD_WS_box = sMTD_WS_box + (sInSoilold*sMTDFraction);

# Runoff out of cells of saturated overlandflow, modified by slope (mm/h)
# a) storage runoff
sQ_SOF = (sMTD_WS_box * cMTD_K_w) * cSlopeFactor;
sMTD_WS_box = max (sMTD_WS_box - sQ_SOF, 0);
#b) plus runoff over limit of cMTD_US(mm/h)
sQ_SOF = sQ_SOF + max (sMTD_WS_box - cMTD_WS, 0);
# Check that storage is not above limit
sMTD_WS_box = min (sMTD_WS_box, cMTD_WS);

# Evaporation out of MTD wet storage
sActET_SOF1 = if (bSOF_zone, min (sMTD_WS_box, (sMTDFraction*sPotET)));

# Calculate new MTD content
sMTD_WS_box = sMTD_WS_box - sActET_SOF1;

# Flow from wet box to dry box (mm/h)
sStorageLeakMTD = min (sMTD_WS_box, cMTD_T);

# Remaining water in wet storage
sMTD_WS_box = sMTD_WS_box - sStorageLeakMTD;

*****
```

```

# Calculate actual evapotranspiration out of soil
*****
# actual ET equals potential ET if certain fraction of field capacity is reached (cLP [-])
sMeanSoilMoisture = (sSoilMoisture + sSoilMoistureAtBegin) / 2;
sFractionOfPotET = sMeanSoilMoisture / (cLP * cFieldCapacity);

sActET = min ((sPotET * sFractionOfPotET), sPotET);

sActET_SOF2 = if (defined (bSOF_zone),sActET);
sActET_SOF2 = min (((1-sMTDFraction)*sPotET),sActET_SOF2);
sActET_SOF = (sActET_SOF1 + sActET_SOF2);

# Calculate new soil moisture content
sSoilMoisture = max ((sSoilMoisture - sActET), 0);
*****
# SOF Dry zone Storage (DS)
*****
# Input of percolated water from wet storage into dry storage (mm)
sMTD_DS_box = sMTD_DS_box + sStorageLeakMTD;

#Fraction of water to dry box (mm)
sToRunoffGenerationMTD = sToRunoffGeneration;

# Add soil moisture to the storage (mm)
sMTD_DS_box = sMTD_DS_box + sToRunoffGenerationMTD;

# Runoff out of dry storage, modified by slope (mm/h)
# a) storage runoff
sQ_MTD_DS = (sMTD_DS_box * cMTD_K_d) * cSlopeFactor;

# Remaining water in storage (mm)
sMTD_DS_box = max(sMTD_DS_box - sQ_MTD_DS, 0);

#b)plus runoff over limit cMTD_DS
sQ_MTD_DS = sQ_MTD_DS + max (sMTD_DS_box - cMTD_DS,0);

# Check that storage is not above limit
sMTD_DS_box = min (sMTD_DS_box, cMTD_DS);

#Calculate the total runoff of the different areas in the riparian zones
sQ_MTD_total = sQ_MTD_DS + sQ_SOF;

*****
# Runoff into stream and lateral flows
*****
# Lateral flows (mm/h)
# a) SOF-zone
sMTD_WS_box = sMTD_WS_box + (sMTDFraction * upstream(LDD, sQ_));

sMTD_DS_box = sMTD_DS_box + (1-sMTDFraction)* upstream(LDD, sQ_);

```

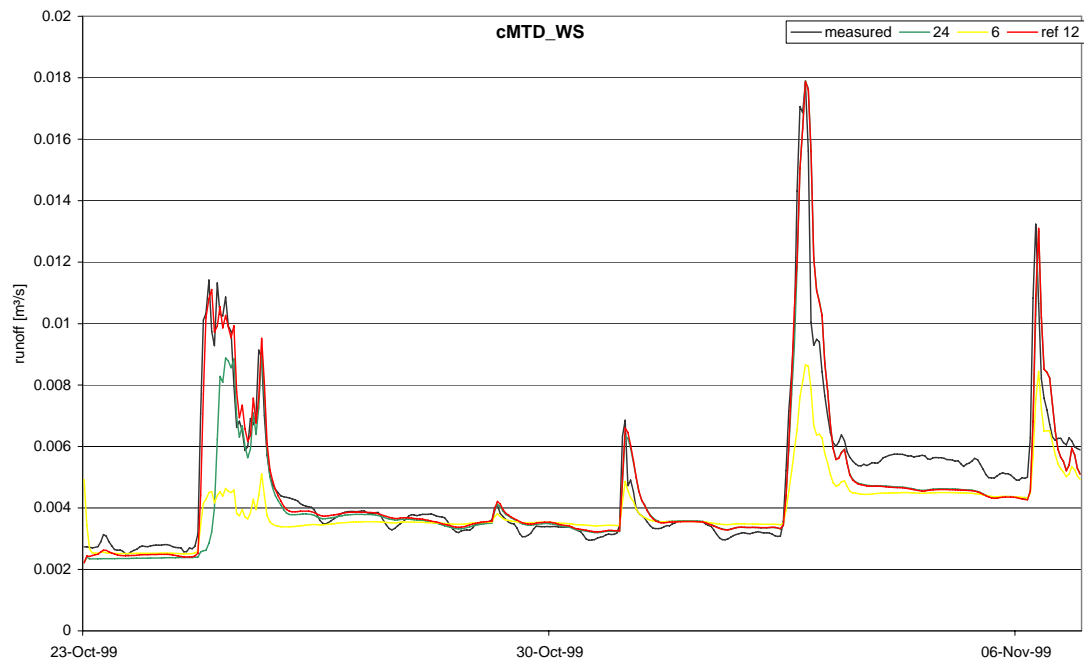
## Annex E Water balances for the different models

Water balance TAC-D with original parameters				
ET [mm]	-141512			
InStream [mm]	-160160	EndStor. [mm]	2188140	
Prec [mm]	1119770	StartStor.[mm]	1370040	<b>Difference</b>
<b>Total</b>	818098	<b>Total</b>	818100	-2

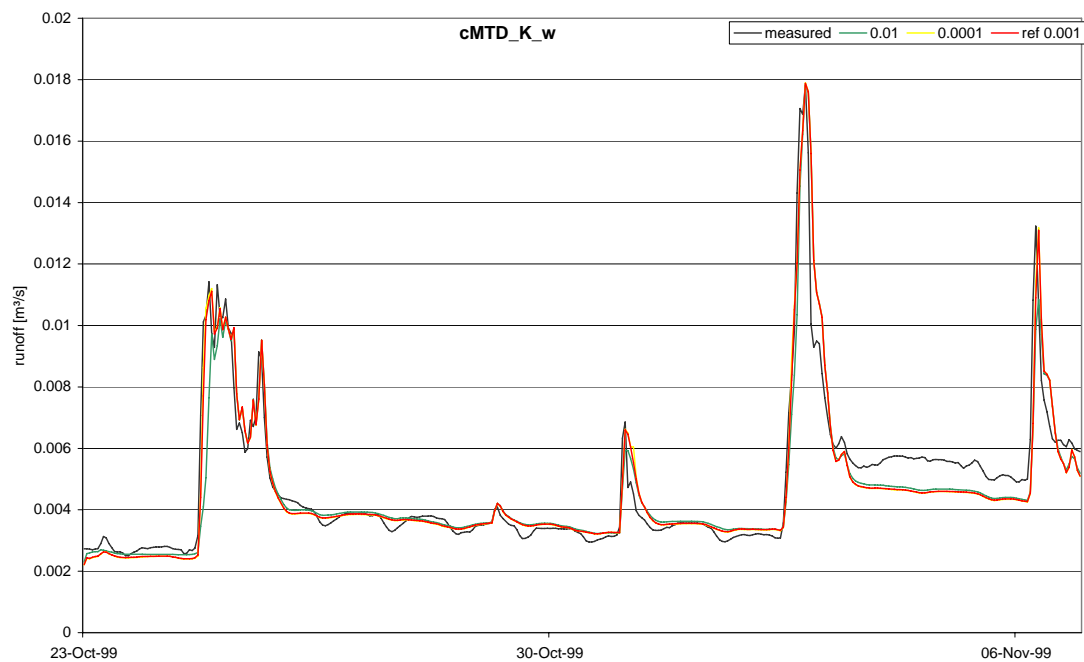
Water balance TAC-D with adjusted parameters				
ET [mm]	-141593			
InStream [mm]	-301283	EndStor. [mm]	2046940	
Prec [mm]	1119770	StartStor.[mm]	1370040	<b>Difference</b>
<b>Total</b>	676894	<b>Total</b>	676900	-6

Water balance TAC-D incl. SVRA-module				
ET [mm]	-141596			
InStream [mm]	-238410	EndStor. [mm]	2142680	
Prec [mm]	1119770	StartStor.[mm]	1402920	<b>Difference</b>
<b>Total</b>	739764	<b>Total</b>	739760	4

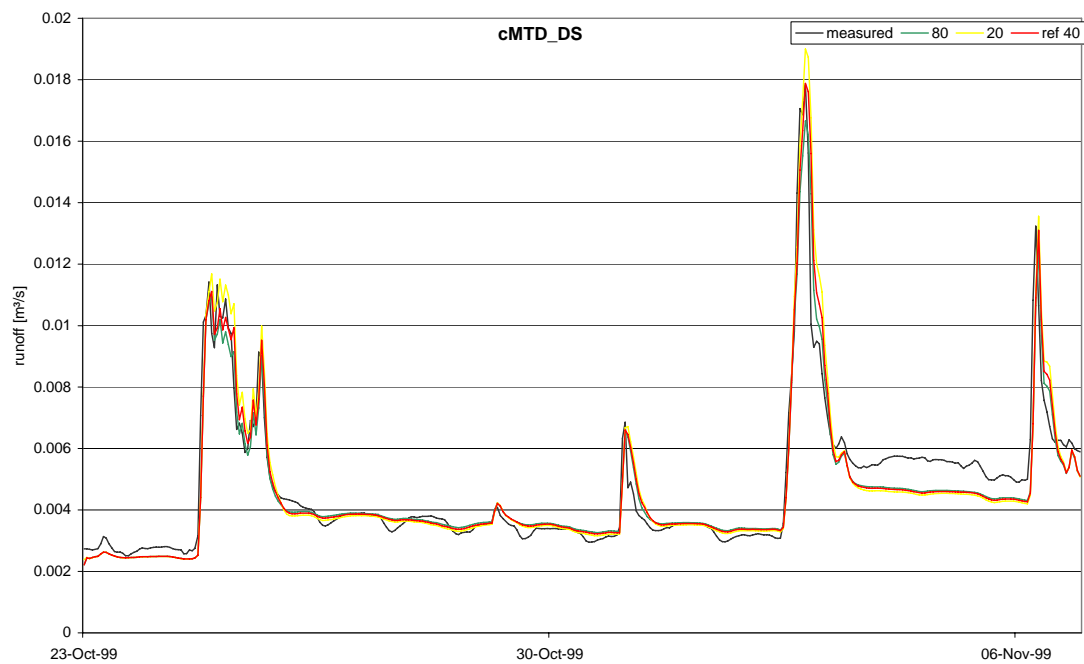
## Annex F Hydrographs of the parameter sensitivity analysis



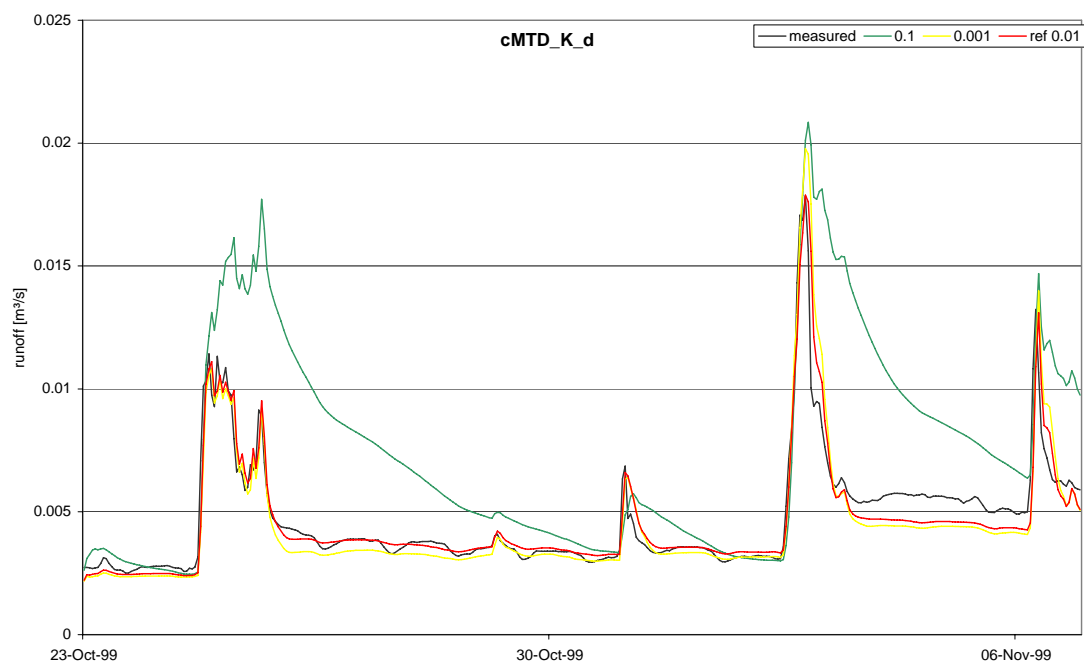
**Sensitivity of the storage capacity of the Wet Storage box of the riparian area on the simulated runoff**



**Sensitivity of the hydraulic conductivity of the Wet Storage box of the riparian area on the simulated runoff**

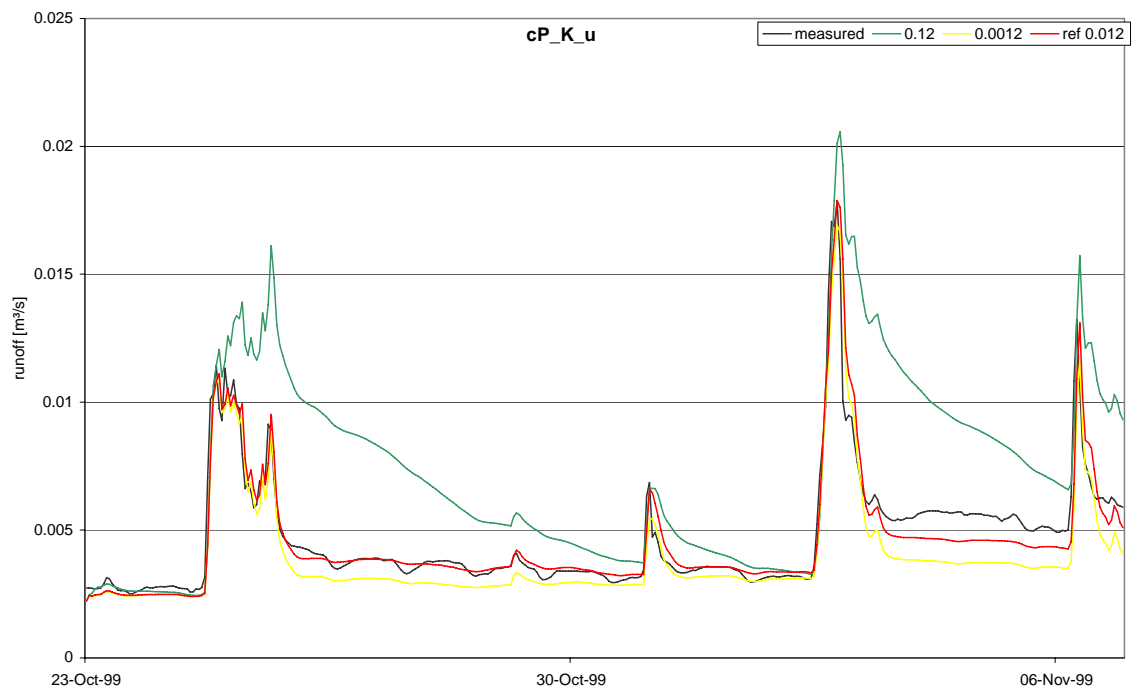


**Sensitivity of the storage capacity of the Dry Storage box of the riparian area on the simulated runoff**

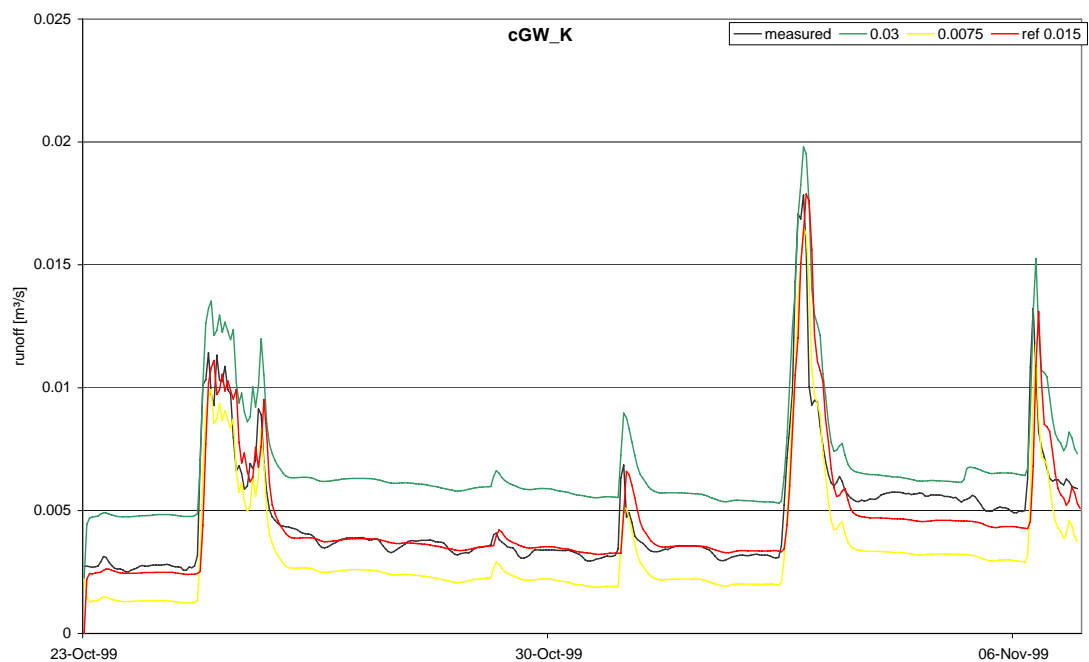


**Sensitivity of the hydraulic conductivity of the Dry Storage box of the riparian area on the simulated runoff**





**Sensitivity of the hydraulic conductivity of the upper storage box of the periglacial cover layer on the simulated runoff**



**Sensitivity of the hydraulic conductivity of the groundwater box on the simulated runoff**

## Annex G Model performance parameters

TAC-D with original parameters	Calculation period		
	Calibration	Validation	Entire
<i>Model efficiency, <math>R_{eff}</math> [-]</i>	0.37	0.03	0.16
<i>Volume error, mean VE [<math>m^3/s</math>]</i>	0.00127	0.0019	0.0016
<i>Volume error, total VE [<math>m^3/s</math>]</i>	0.2026	0.3859	0.5886
<i>Absolute mean VE [<math>m^3/s</math>]</i>	0.0017	0.0023	0.0021
<i>Absolute total VE [<math>m^3/s</math>]</i>	0.2712	0.4677	0.7389
<i>VE [%]</i>	40.4	45.4	43.5

TAC-D with calibrated parameters	Calculation period		
	Calibration	Validation	Entire
<i>Model efficiency, <math>R_{eff}</math> [-]</i>	0.39	0.34	0.36
<i>Volume error, mean VE [<math>m^3/s</math>]</i>	-0.00001	0.0001	0.0001
<i>Volume error, total VE [<math>m^3/s</math>]</i>	0.0001	0.0253	0.0230
<i>Absolute mean VE [<math>m^3/s</math>]</i>	0.0008	0.0008	0.0008
<i>Absolute total VE [<math>m^3/s</math>]</i>	0.1274	0.1575	0.2850
<i>VE [%]</i>	19.0	15.3	16.8

TAC-D including SVRA-module with calibrated parameters	Calculation period		
	Calibration	Validation	Entire
<i>Model efficiency, <math>R_{eff}</math> [-]</i>	0.944	0.927	0.933
<i>Volume error, mean VE [<math>m^3/s</math>]</i>	0.0001	0.0002	0.0001
<i>Volume error, total VE [<math>m^3/s</math>]</i>	0.0108	0.0347	0.0455
<i>Absolute mean VE [<math>m^3/s</math>]</i>	0.0003	0.0006	0.0005
<i>Absolute total VE [<math>m^3/s</math>]</i>	0.0463	0.1282	0.1744
<i>VE [%]</i>	6.9	12.5	10.3